

**Polycationic Monomeric and Homodimeric Asymmetric Monomethine Cyanine dyes with
Hydroxypropyl Functionality – Strong Affinity Nucleic Acids Binders**

Ivana Mikulin^{a#}, Ivana Sorić^{a#}, Ivo Piantanida^a, Aleksey Vasilev^{b*}, Mihail Mondeshki^d, Meglena Kandinska^b, Lidija Uzelac^c, Irena Martin-Kleiner^c, Marijeta Kralj^c, Lidija-Marija Tumir^{a*}

^aLaboratory for Biomolecular Interactions and Spectroscopy, Division of Organic Chemistry and Biochemistry, Ruđer Bošković Institute, HR 10002 Zagreb, P.O.B. 180, Croatia, E-mail: tumir@irb.hr

^bDepartment of Pharmaceutical and Applied Organic Chemistry, Faculty of Chemistry and Pharmacy, Sofia University “St. Kliment Ohridski”, Sofia, Bulgaria, E-mail: ohtavv@chem.uni-sofia.bg

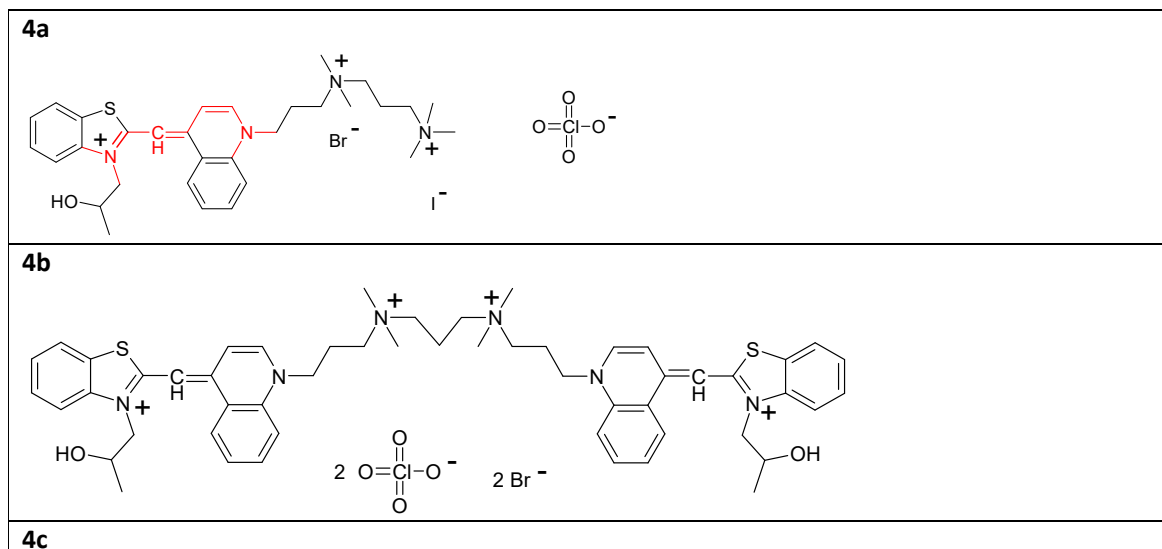
^c Laboratory of Experimental Therapy, Division of Molecular Medicine, Ruđer Bošković Institute, HR 10002 Zagreb, P.O.B. 180, Croatia

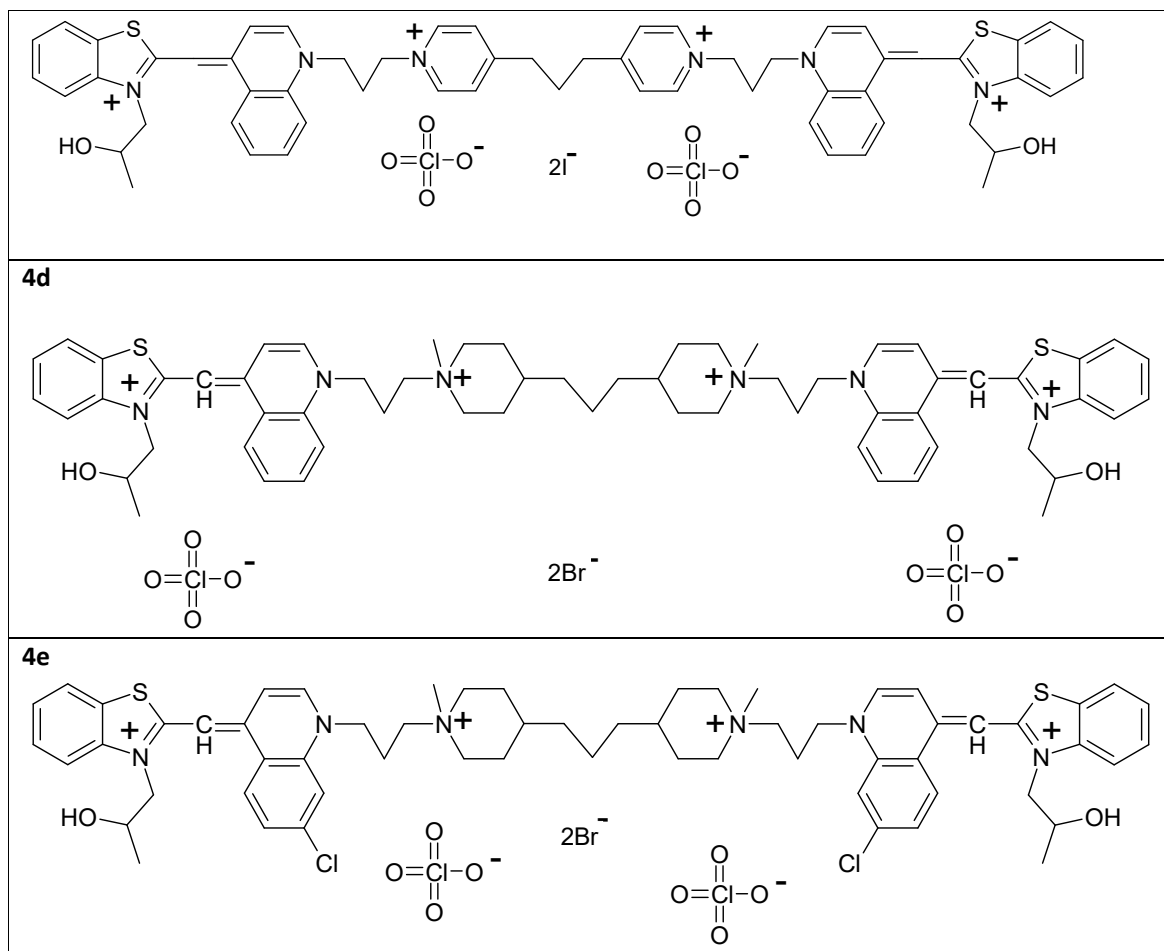
^d Department of Chemistry, Johannes Gutenberg Universität Mainz, Duesbergweg 10-14, 55128 Mainz, Germany

#equal contribution

Supporting Information

1. Spectroscopic properties of **4a-4e** compounds
2. Interactions of **4a-4e** compounds with DNA/RNA
3. Biology





Scheme S1. Structures of examined **4a-4e** compounds

1. Spectroscopic properties of **4a-4e** compounds

Absorption maxima and corresponding molar extinction coefficients (ε) are given in Table S1 and Figure S1.

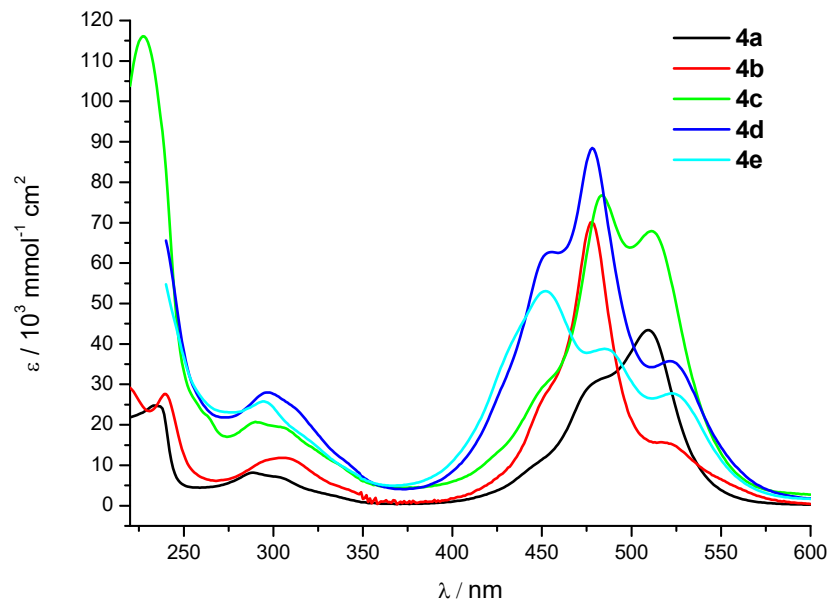


Figure S1. UV/Vis spectra of **4a-4e** at pH=7, sodium cacodylate/HCl buffer, $I = 0.05 \text{ mol dm}^{-3}$.

Table S1. Electronic absorption data of **4a-4e** (Sodium cacodylate buffer, $I = 0.05 \text{ mol dm}^{-3}$, pH = 7.)

	$\lambda_{\max} / \text{nm}$	$\varepsilon / \text{mmol}^{-1} \text{cm}^2$
4a	235	25062
	478	31079
	509	44971
4b	239	34818
	478	70024
	509	15982
4c	227	115617
	484	76515
	511	67971
4d	296	28848
	455	63848
	478	84394
	521	36220
4e	294	25736
	452	53588
	486	39230
	523	27929

2. Study of interactions of **4a - 4e** with ds-DNA and ds-RNA in aqueous media

Table S2. Groove widths and depths for selected nucleic acid conformations ¹

	Groove width [Å]		Groove depth [Å]	
	minor	major	minor	major

^a poly dAdT – poly dAdT	6.3	11.2	7.5	8.5
^a poly dA – poly dT	3.3	11.4	7.9	7.5
^b poly rA- poly rU	10.9	3.8	2.8	13.5
^a poly dGdC – poly dGdC	9.5	13.5	7.2	10.0

^a B-helical structure (e.g. B-DNA); ^b A-helical structure (e.g. A-DNA or A-RNA).

2.1. Thermal melting experiments

All thermal melting experiments were performed sodium cacodylate buffer, pH = 7.0, $I = 0.05 \text{ mol dm}^{-3}$; c (polynucleotide) = $1\text{-}2 \times 10^{-5} \text{ mol dm}^{-3}$

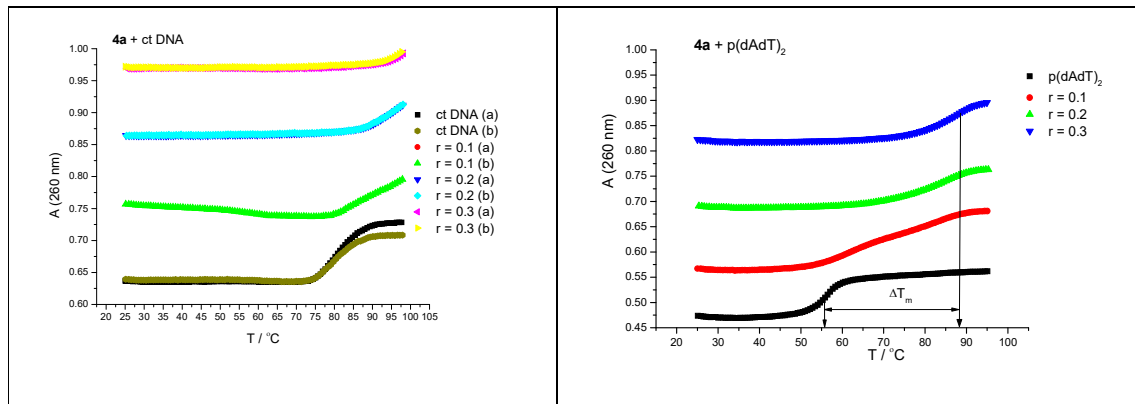


Figure S2. Normalized melting curves of ct DNA (left) and poly dAdT – poly dAdT (right) upon addition of **4a** (ratios r =[compound] / [polynucleotide] indicated in the graph legend.

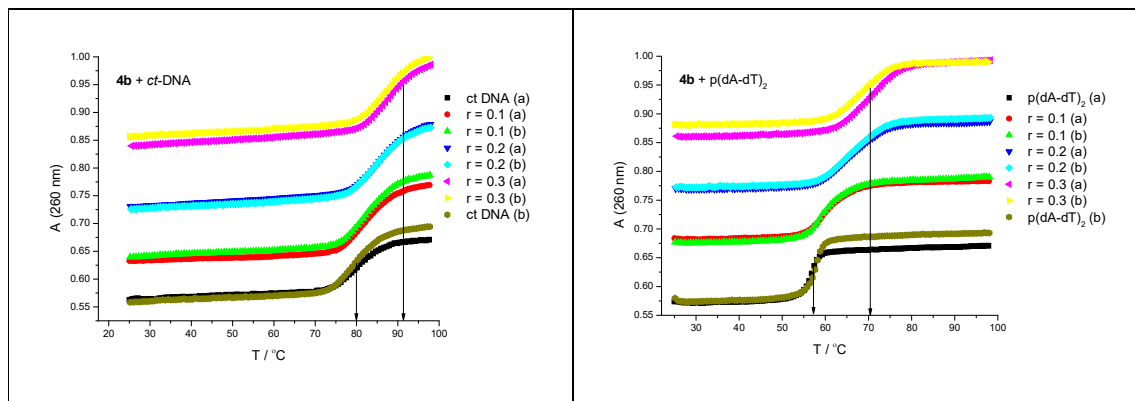


Figure S3. Normalized melting curves of ct DNA (left) and poly dAdT – poly dAdT (right) upon addition of **4b** (ratios r =[compound] / [polynucleotide] indicated in the graph legend.

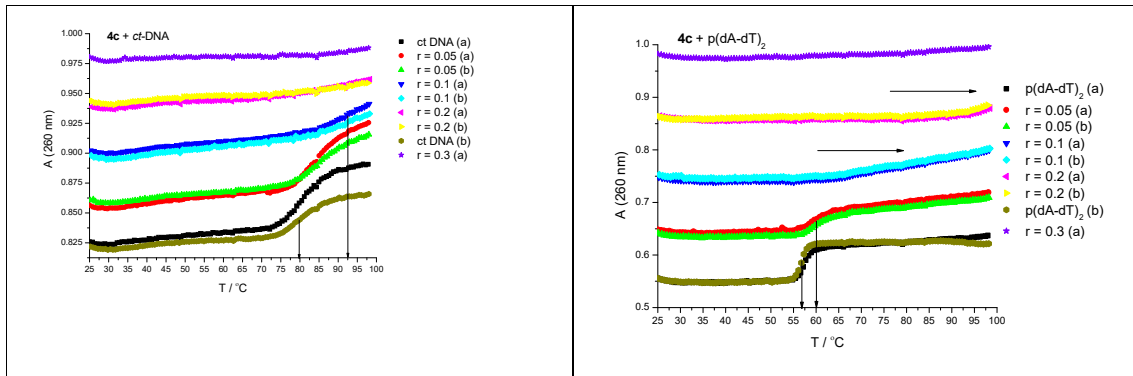


Figure S4. Normalized melting curves of ct DNA (left) and poly dAdT – poly dAdT (right) upon addition of **4c** (ratios r =[compound] / [polynucleotide] indicated in the graph legend).

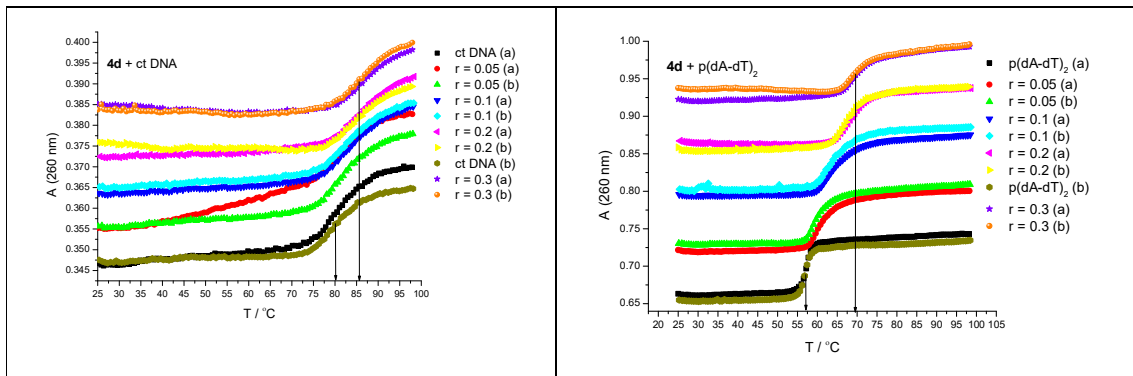


Figure S5. Normalized melting curves of ct DNA (left) and poly dAdT – poly dAdT (right) upon addition of **4d** (ratios r =[compound] / [polynucleotide] indicated in the graph legend).

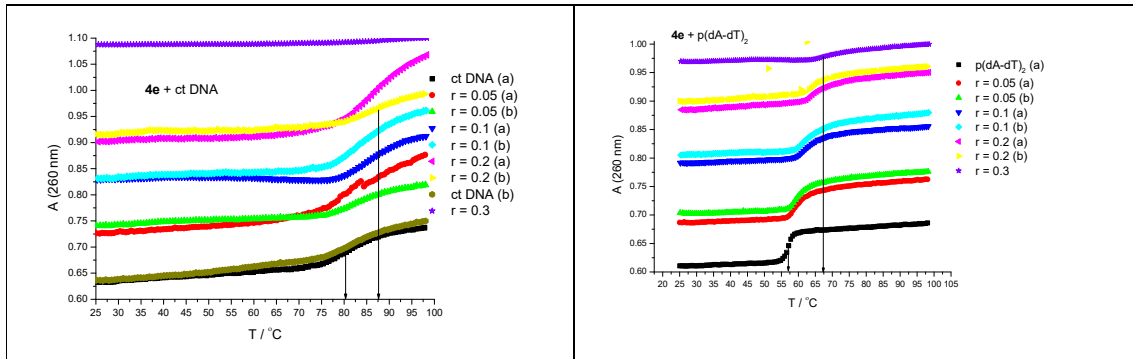


Figure S6. Normalized melting curves of ct DNA (left) and poly dAdT – poly dAdT (right) upon addition of **4e** (ratios r =[compound] / [polynucleotide] indicated in the graph legend).

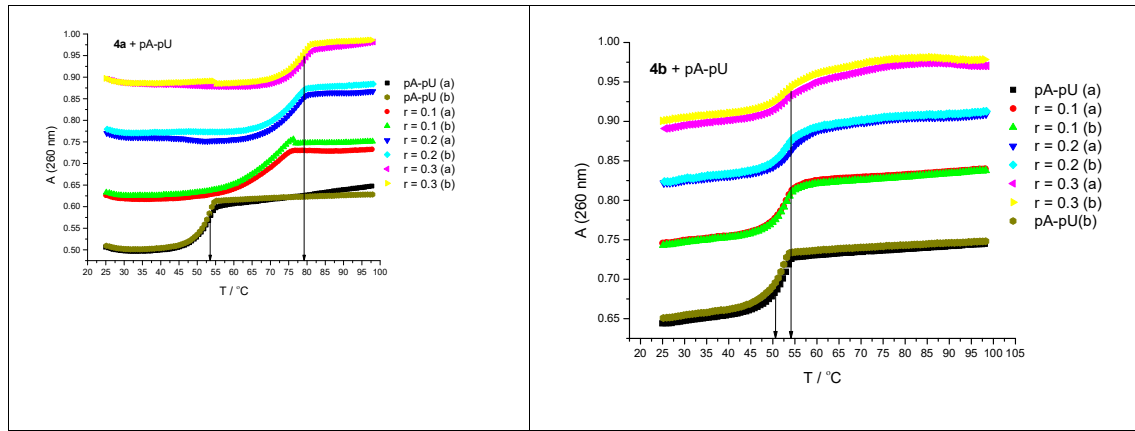


Figure S7. Normalized melting curves of poly rA – poly rU upon addition of **4a** (left) and **4b** (right) (ratios r =[compound] / [polynucleotide] indicated in the graph legend).

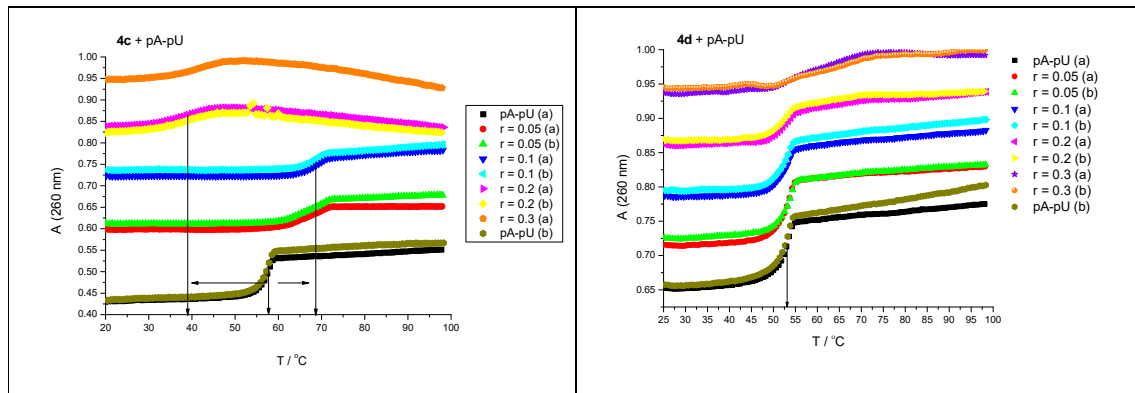


Figure S8. Normalized melting curves of poly rA – poly rU upon addition of **4c** (left) and **4d** (right) (ratios r =[compound] / [polynucleotide] indicated in the graph legend).

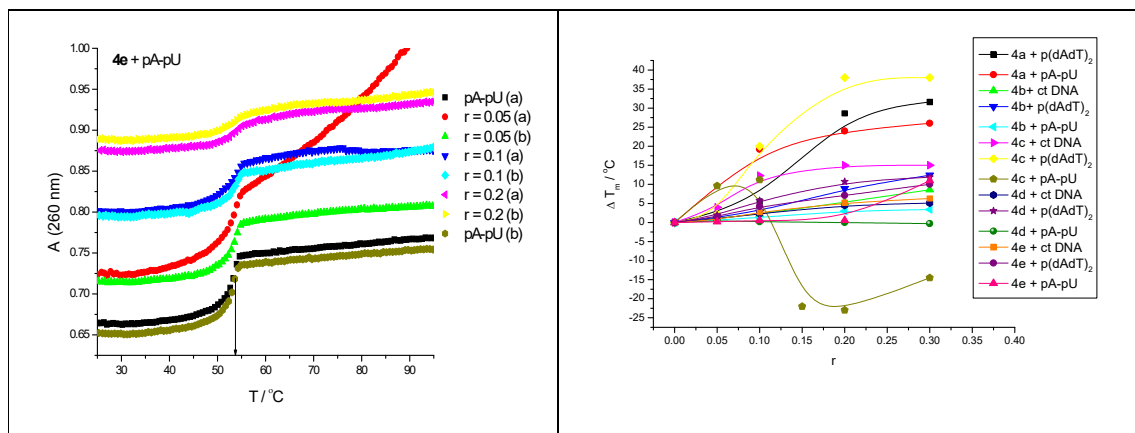
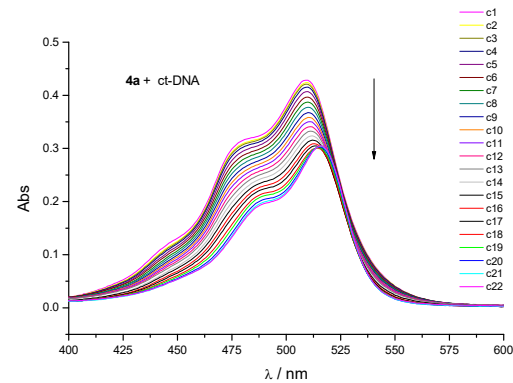


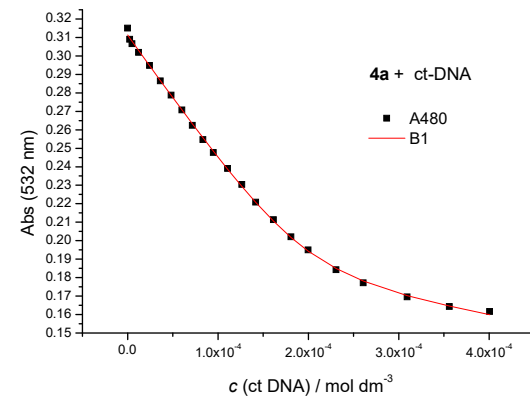
Figure S9. Left: Normalized melting curves of poly rA – poly rU upon addition of **4e** (ratios r =[compound] / [polynucleotide] indicated in the graph legend. Right: Correlation of ΔT_m values and ratios r [compound] / [polynucleotide] for complexes of examined compounds with different polynucleotides.

2.2. Spectrophotometric titrations

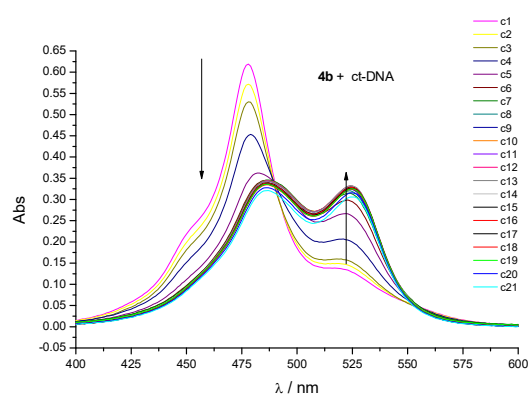
Addition of *ct*-DNA resulted in strong bathochromic and hypochromic effects of UV/Vis spectra of studied compounds (Figure S10, spectral changes observed in UV/Vis titrations for all compounds are summarized in Table S3). All UV-Vis titrations were performed at pH=7, sodium cacodylate buffer, $I = 0.05 \text{ mol dm}^{-3}$.



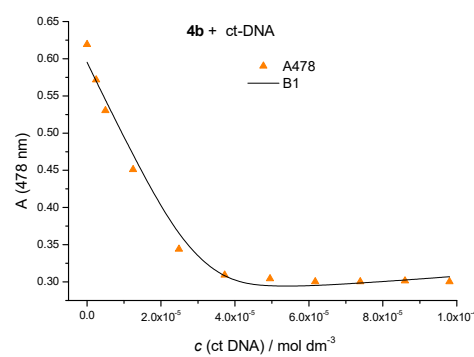
a1)



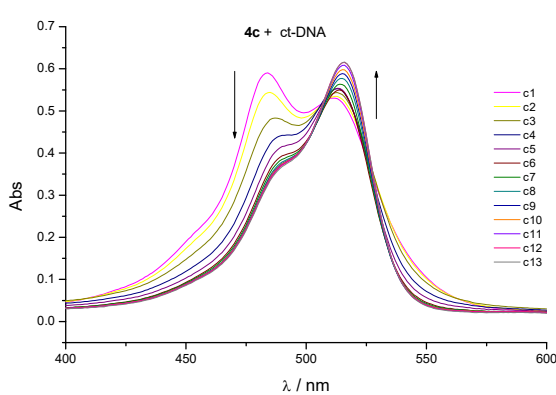
a2)



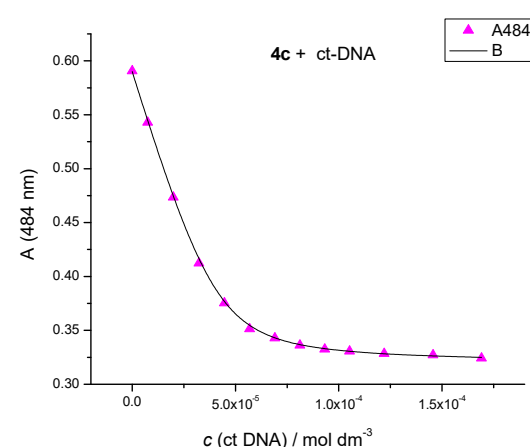
b1)



b2)



c1)



c2)

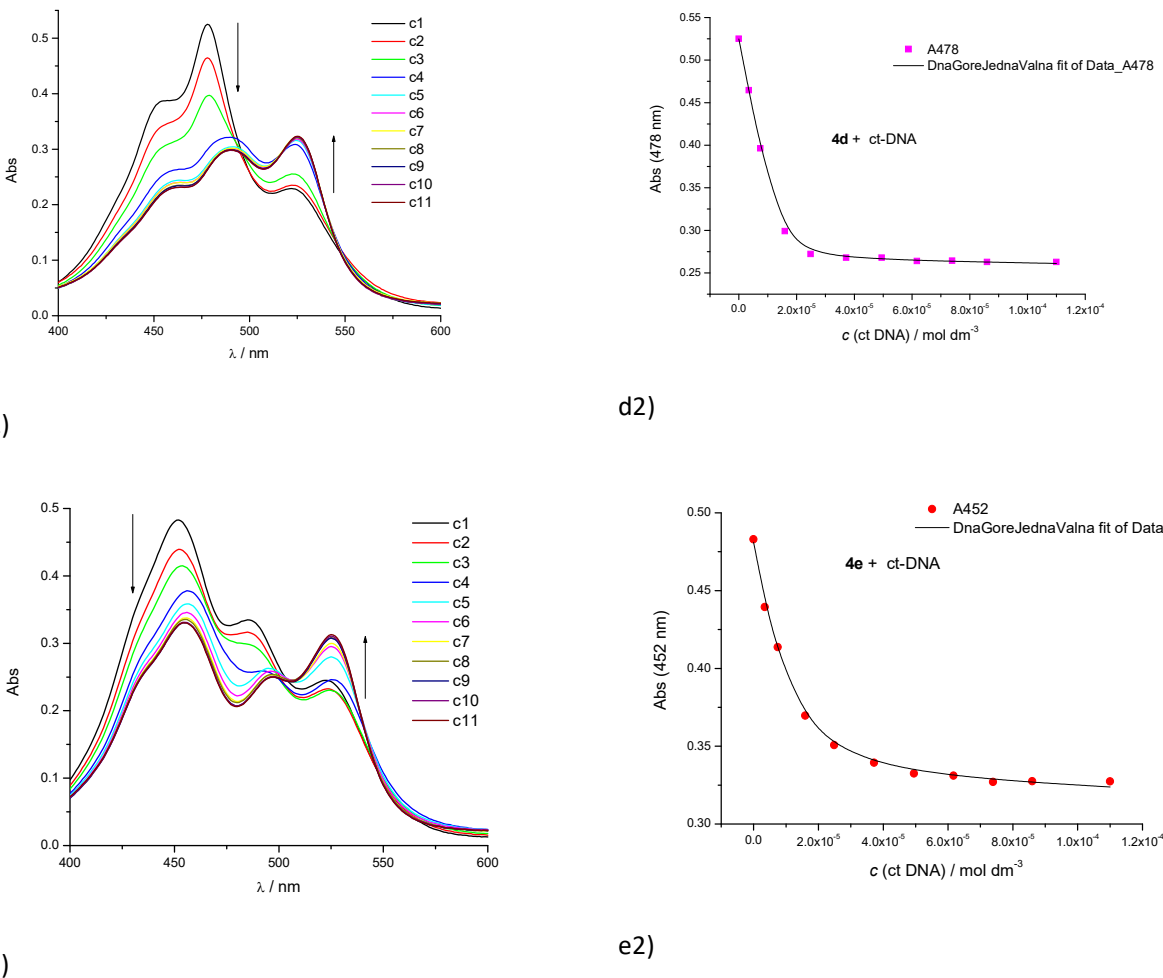


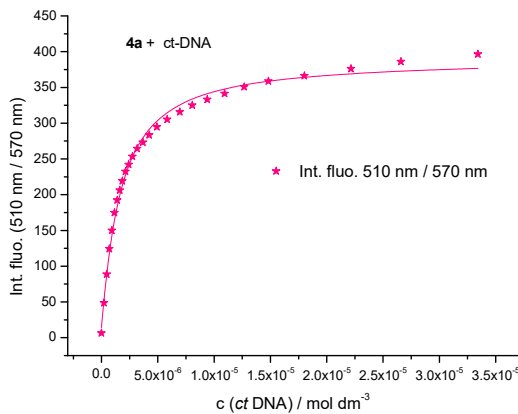
Figure S10. Changes in UV-Vis spectra upon addition of *ct*-DNA: a1) UV/Vis titration of **4a** ($c = 1.11 \times 10^{-5}$ mol dm $^{-3}$); a2) changes in UV/Vis spectra of **4a** at $\lambda = 480$ nm b1) UV/Vis titration of **4b** ($c = 8.03 \times 10^{-6}$ mol dm $^{-3}$); b2) Changes in UV/Vis spectra of **4b** at $\lambda_{\text{max}} = 519$ nm; c1) UV/Vis titration of **4c** ($c = 7.41 \times 10^{-6}$ mol dm $^{-3}$); c2) Changes in UV/Vis spectra of **4c** at $\lambda_{\text{max}} = 484$ nm, d1) UV/Vis titration of **4d** ($c = 8.03 \times 10^{-6}$ mol dm $^{-3}$); d2) Changes in UV/Vis spectra of **4d** at $\lambda_{\text{max}} = 478$ nm; e1) UV/Vis titration of **4e** ($c = 9 \times 10^{-6}$ mol dm $^{-3}$); e2) Changes in UV/Vis spectra of **4e** at $\lambda_{\text{max}} = 452$ nm.

Table S3. Apparent stability constants ($\log K_s$)^a, ratios $n^a = [\text{bound compounds}] / [\text{polynucleotide}]$ and spectroscopic properties of complexes of **4a** - **4e** with *ct*-DNA calculated according to UV-Vis titrations (Na-cacodylate buffer, $c = 0.05$ mol dm $^{-3}$, pH = 7.0, $\lambda = 400$ -600 nm, $c(4a) \approx 1 \times 10^{-5}$ mol dm $^{-3}$).

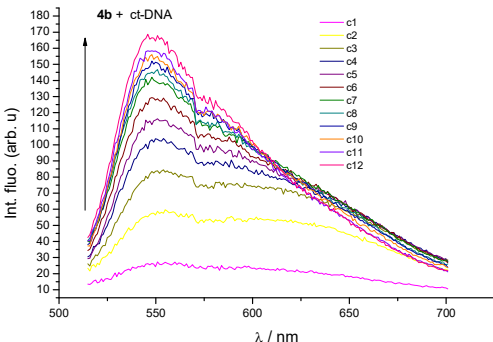
	$\log K_s$	n	$\Delta A (\%)^b$	$\Delta\lambda / \text{nm}^c$
4a	6.28	0.05	-40%	+7
4b	5.99	0.26	-50%	+10
4c	6.37	0.18	-44%	+10
4d	6.65	0.42	-50%	+12
4e	6.02	0.28	-50%	+4

^aTitration data were processed using Scatchard equation²; coefficients of correlation were >0.989-0.999 for all calculated *K*s; ^bChanges of absorbance of compounds **4a** - **4e** induced by complex formation ($\Delta A = 100 \times (A_{\text{lim}} - A_0) / A_0$; A_0 is calculated absorbance of examined compound, while A_{lim} is calculated absorbance of complex); ^cChanges of wavelength of absorbance maxima $\Delta\lambda = \lambda_{\text{max}}(\text{complex}) - \lambda_{\text{max}}(\text{pure compound})$; referring to absorption maxima 478-485 nm.

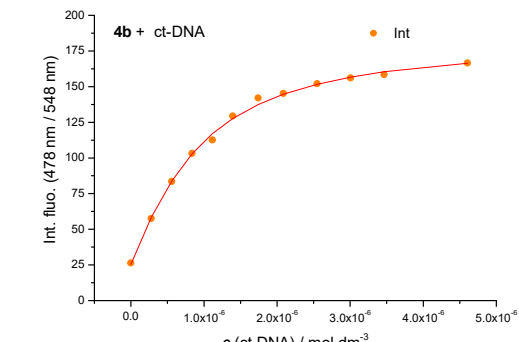
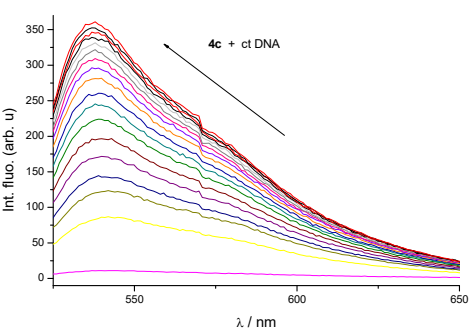
All fluorimetric titrations (Figure S11-Figure S17) were performed at pH=7, sodium cacodylate buffer, $I = 0.05 \text{ mol dm}^{-3}$ at the wavelength range ($\lambda_{\text{exc}}=480-510 \text{ nm}$, $\lambda_{\text{em}}=525-650 \text{ nm}$) significantly distanced from the absorbance range of the DNA/RNA ($\lambda=220-300 \text{ nm}$). Stability constants (manuscript, Table 2) and calculated intensities were obtained by means of Scatchard equation².



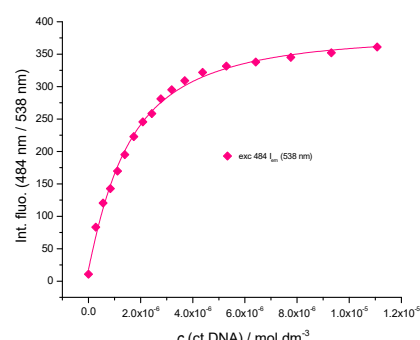
a1)



b1)



b2)



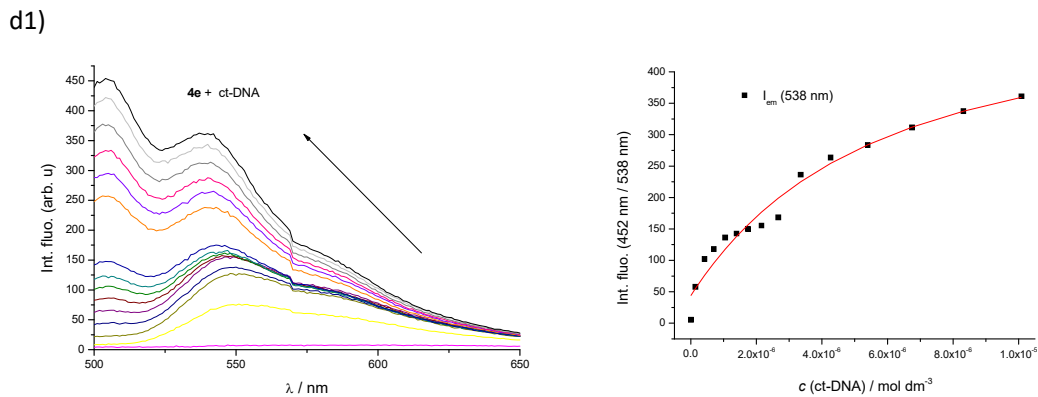
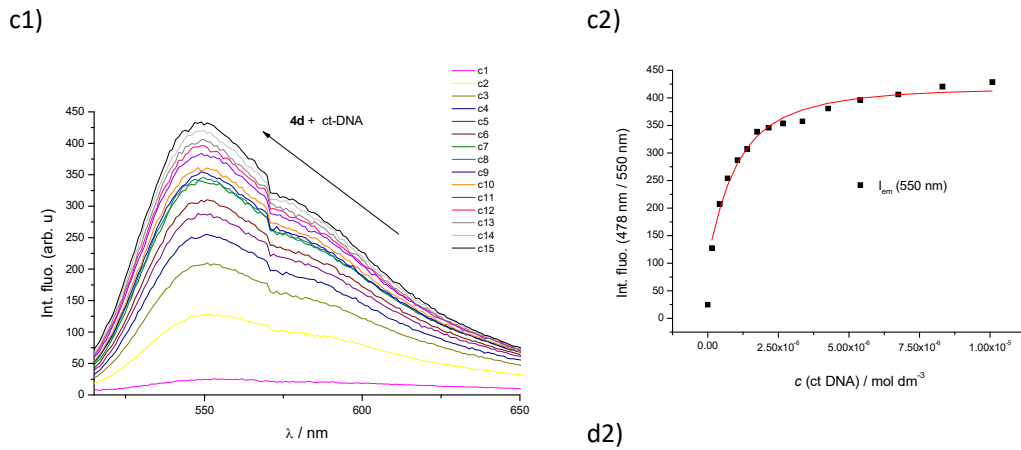
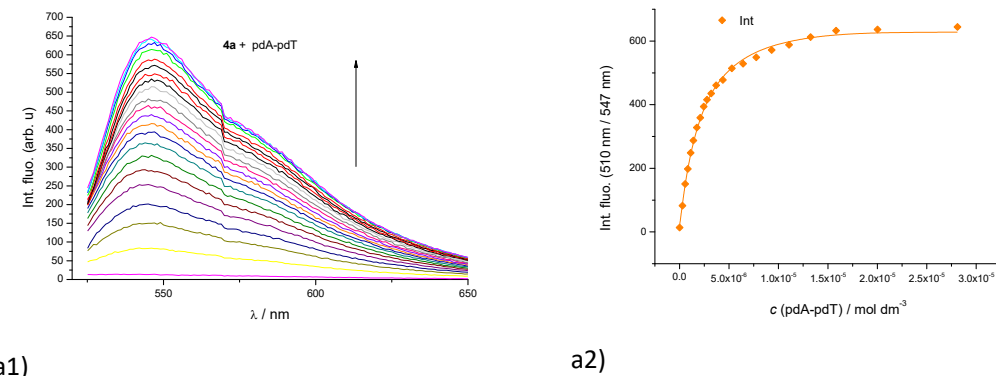
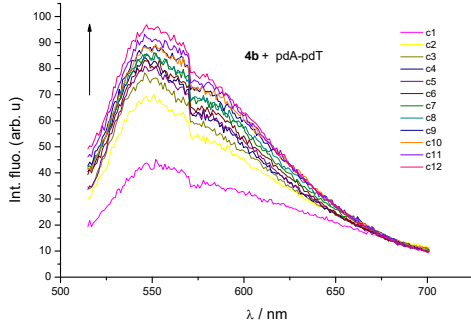
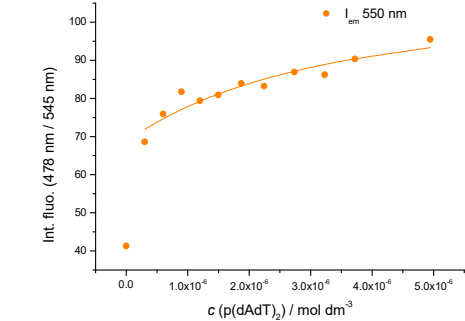
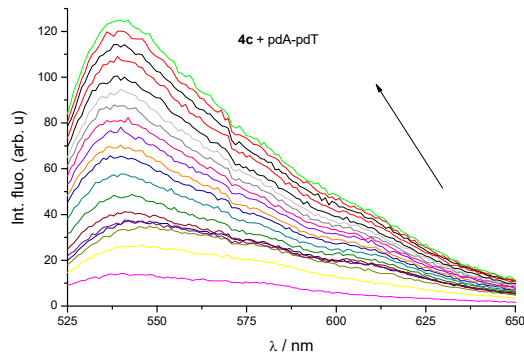


Figure S11. Fluorimetric titration of **4a-4e** compounds ($c = 1.3-1.5 \times 10^{-7} \text{ mol dm}^{-3}$) with **ct-DNA**: a1) Experimental (●) and calculated (—) fluorescence intensities of **4a** at $\lambda_{\text{em}} = 570 \text{ nm}$ **4a** ($\lambda_{\text{exc}}=510 \text{ nm}$); b1) Fluorimetric titration of **4b** ($\lambda_{\text{exc}}=478 \text{ nm}$); b2) Experimental (●) and calculated (—) fluorescence intensities of **4b** at $\lambda = 548 \text{ nm}$; c1) **4c** ($\lambda_{\text{exc}}=484 \text{ nm}$); c2) Experimental (●) and calculated (—) fluorescence intensities of **4c** at $\lambda = 538 \text{ nm}$; d1) **4d** ($\lambda_{\text{exc}}=484 \text{ nm}$); d2) Experimental (●) and calculated (—) fluorescence intensities of **4d** at $\lambda = 550 \text{ nm}$; e1) **4e** ($\lambda_{\text{exc}}=452 \text{ nm}$) e2) Experimental (●) and calculated (—) fluorescence intensities of **4e** at $\lambda = 538 \text{ nm}$

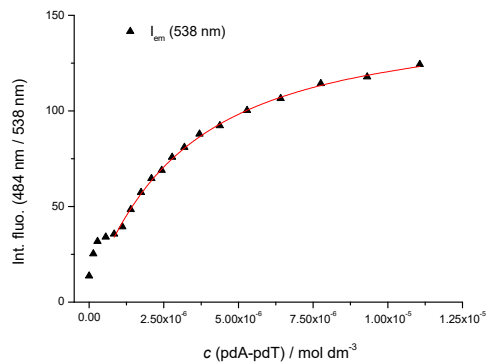




b1)

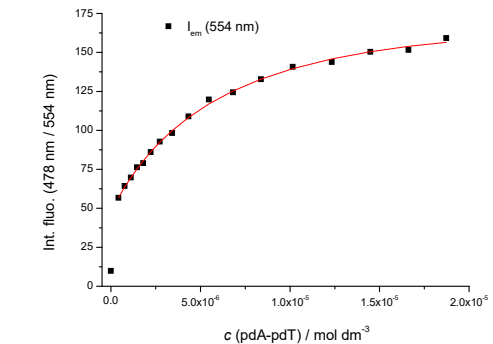
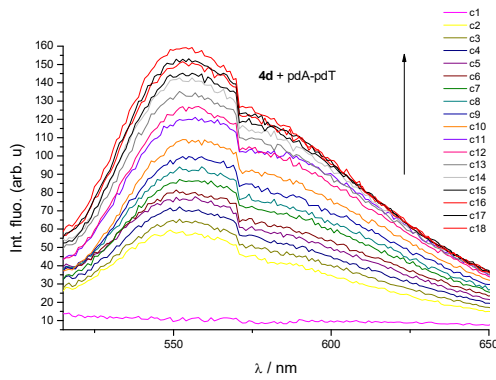


b2)



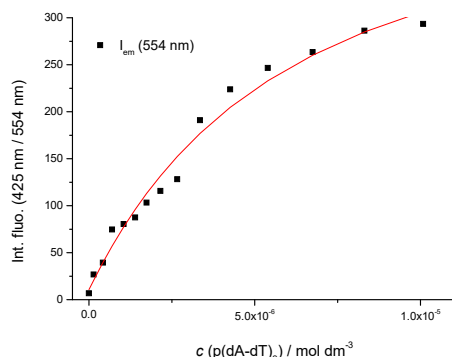
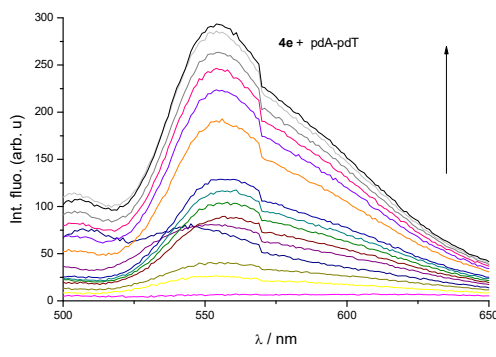
c2)

c1)



d2)

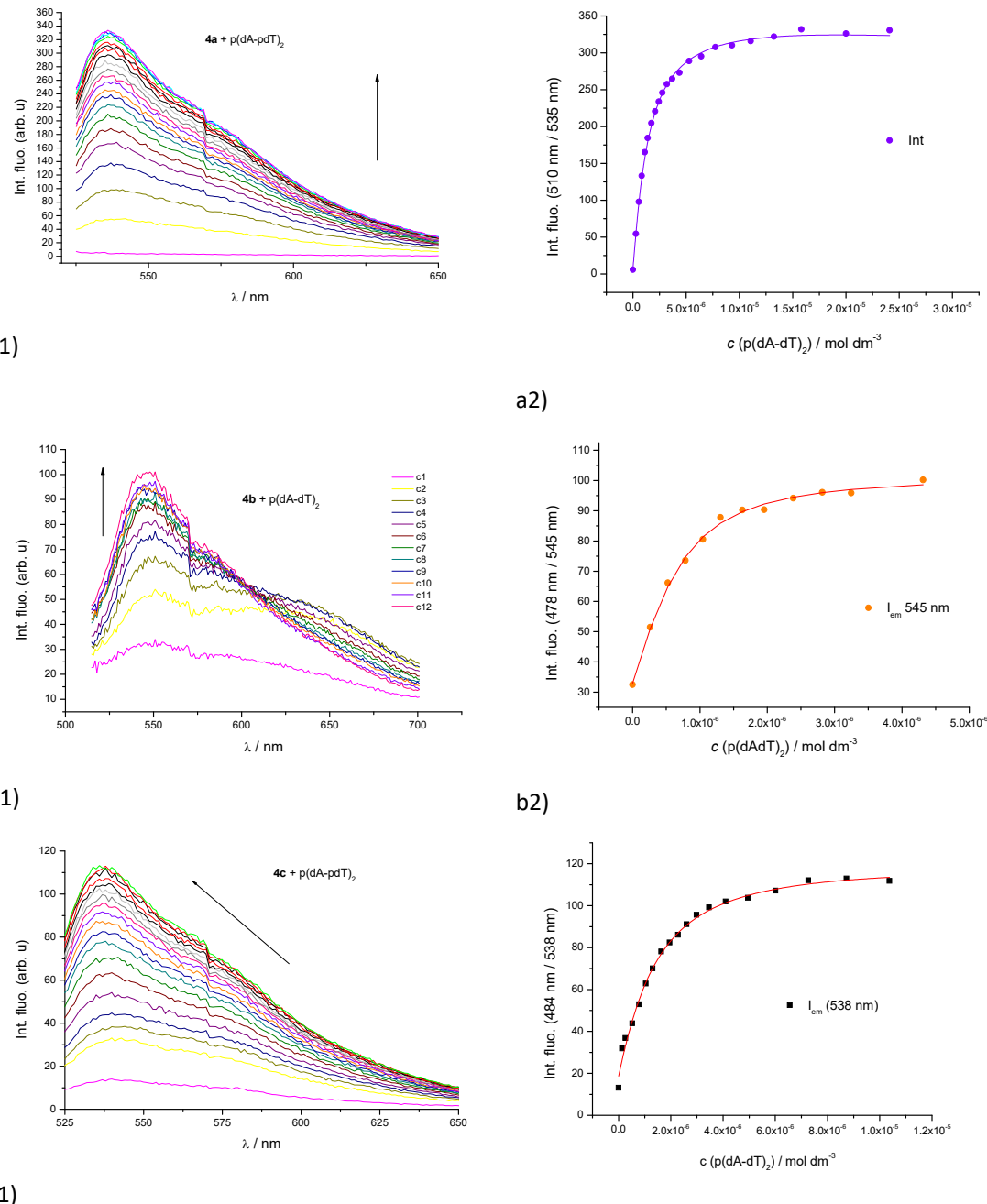
d1)



e1)

e1)

Figure S12. Fluorimetric titration of **4a-4e** compounds ($c = 1.3\text{-}1.5 \times 10^{-7} \text{ mol dm}^{-3}$) with poly dA – poly dT: a1) **4a** ($\lambda_{\text{exc}}=510 \text{ nm}$); a2) Experimental (●) and calculated (—) fluorescence intensities of **4a** at $\lambda_{\text{em}} = 547 \text{ nm}$; b1) Fluorimetric titration of **4b** ($\lambda_{\text{exc}}=478 \text{ nm}$); b2) Experimental (●) and calculated (—) fluorescence intensities of **4b** at $\lambda = 545 \text{ nm}$; c1) **4c** ($\lambda_{\text{exc}}=484 \text{ nm}$); c2) Experimental (●) and calculated (—) fluorescence intensities of **4c** at $\lambda = 538 \text{ nm}$; d1) **4d** ($\lambda_{\text{exc}}=484 \text{ nm}$); d2) Experimental (●) and calculated (—) fluorescence intensities of **4d** at $\lambda = 554 \text{ nm}$; e1) **4e** ($\lambda_{\text{exc}}=452 \text{ nm}$); e2) Experimental (●) and calculated (—) fluorescence intensities of **4e** at $\lambda = 554 \text{ nm}$



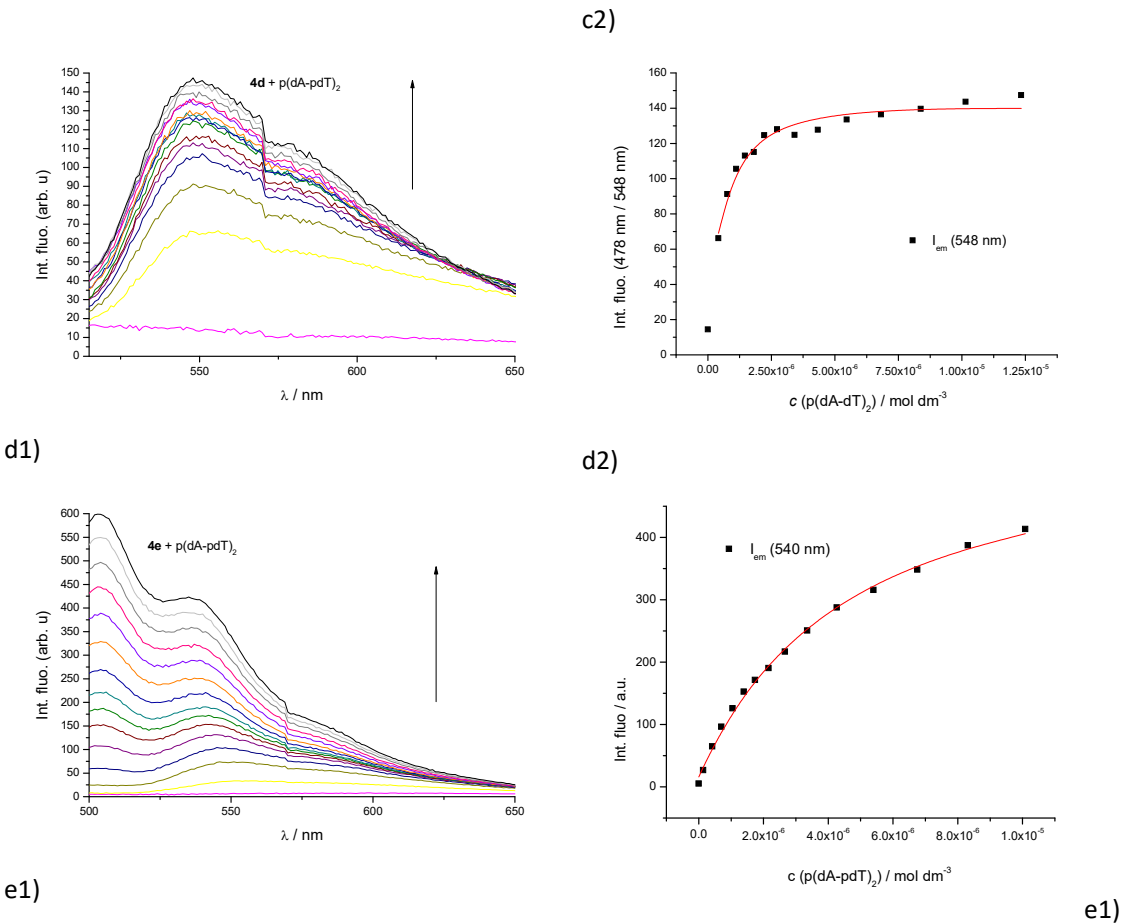
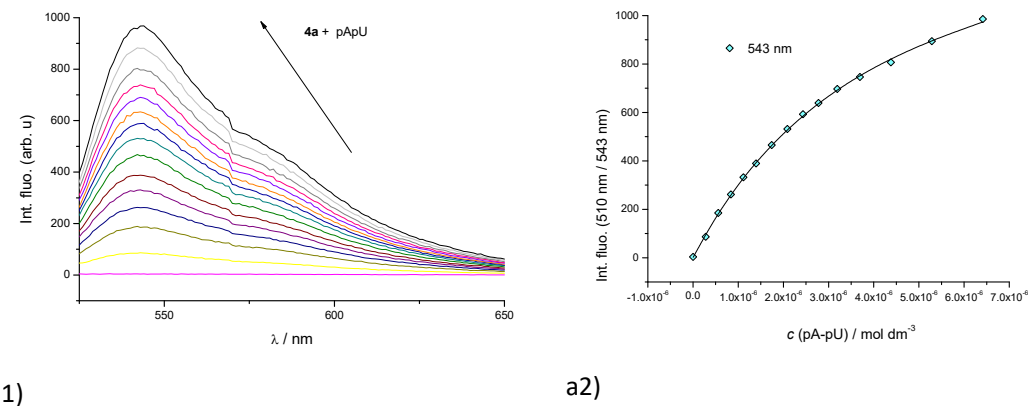
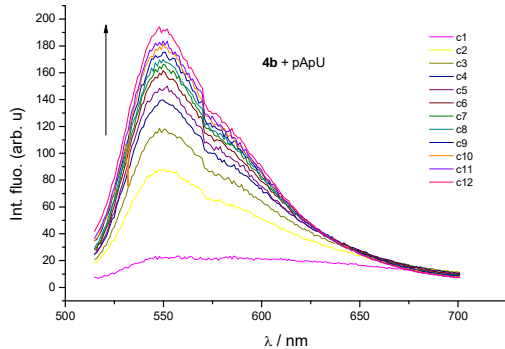
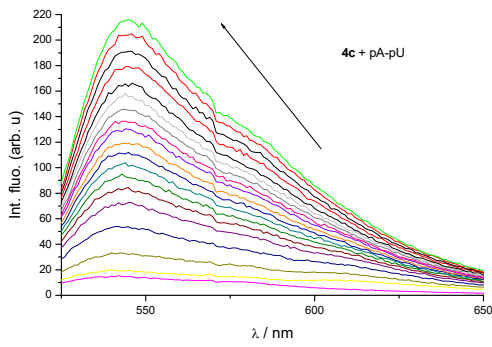


Figure S13. Fluorimetric titration of **4a-4e** compounds ($c = 1.3\text{-}1.5 \times 10^{-7}$ mol dm $^{-3}$) with **poly dAdT** – **poly dAdT**: a1) **4a** ($\lambda_{\text{exc}}=510$ nm); a2) Experimental (\bullet) and calculated (–) fluorescence intensities of **4a** at $\lambda_{\text{em}} = 535$ nm; b1) Fluorimetric titration of **4b** ($\lambda_{\text{exc}}=478$ nm); b2) Experimental (\bullet) and calculated (–) fluorescence intensities of **4b** at $\lambda = 545$ nm; c1) **4c** ($\lambda_{\text{exc}}=484$ nm); c2) Experimental (\bullet) and calculated (–) fluorescence intensities of **4c** at $\lambda = 538$ nm; d1) **4d** ($\lambda_{\text{exc}}=484$ nm); d2) Experimental (\bullet) and calculated (–) fluorescence intensities of **4d** at $\lambda = 548$ nm; e1) **4e** ($\lambda_{\text{exc}}=452$ nm) e2) Experimental (\bullet) and calculated (–) fluorescence intensities of **4e** at $\lambda = 540$ nm

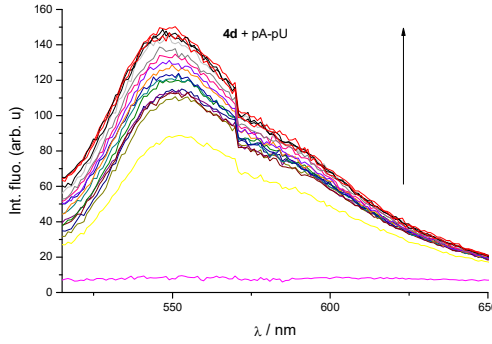




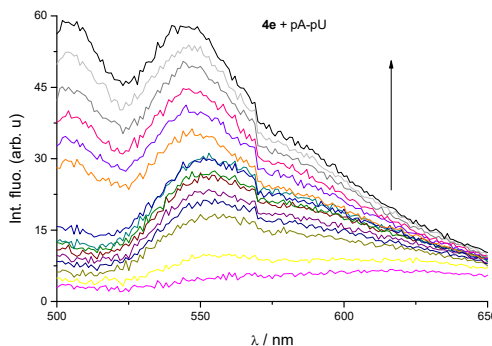
b1)



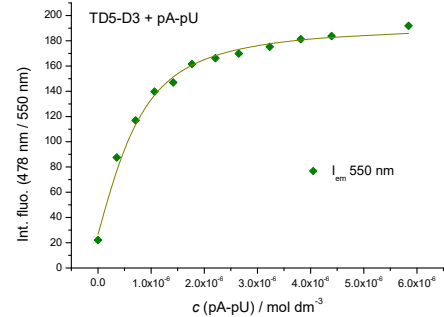
c1)



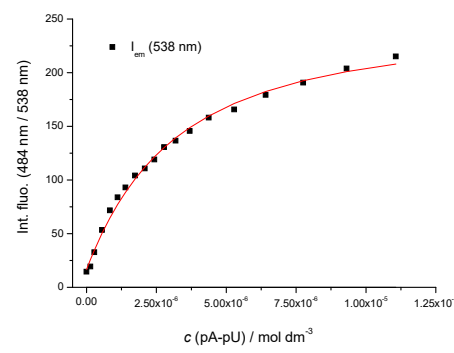
d1)



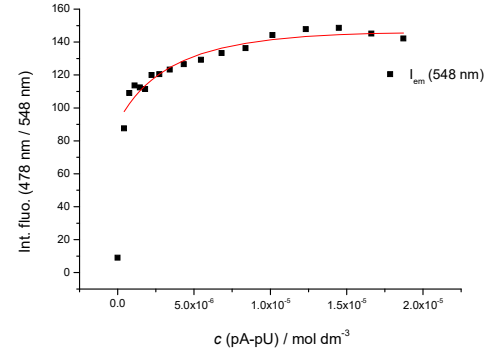
e1)



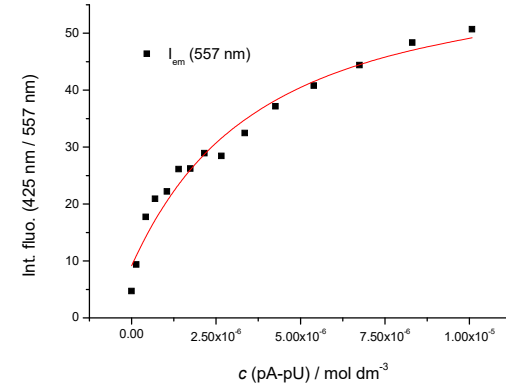
b2)



c2)

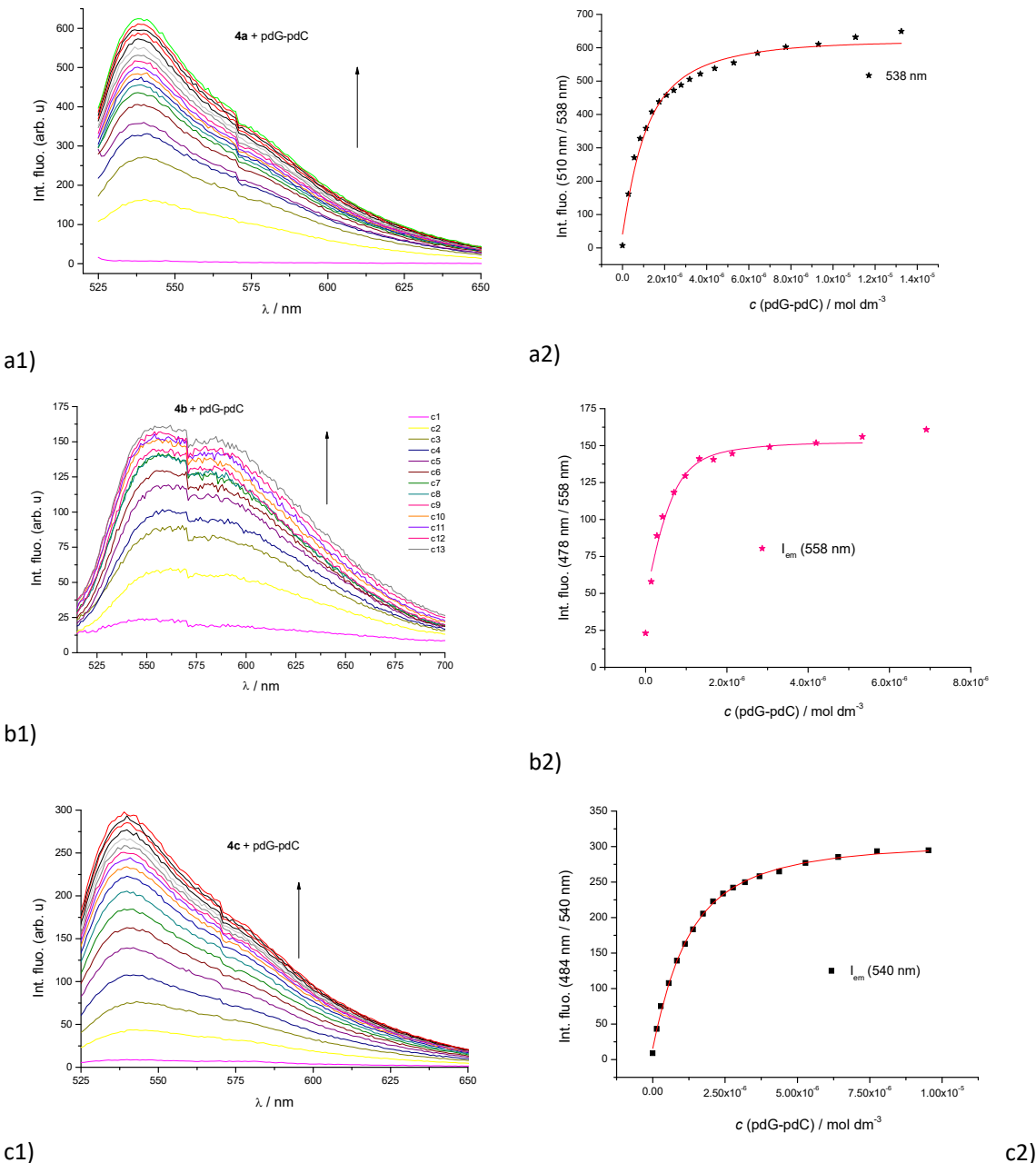


d2)



e1)

Figure S14. Fluorimetric titration of **4a-4e** compounds ($c = 1.3\text{-}1.5 \times 10^{-7}$ mol dm $^{-3}$) with **poly rA – poly rU**: a1) **4a** ($\lambda_{\text{exc}}=510$ nm); a2) Experimental (●) and calculated (—) fluorescence intensities of **4a** at $\lambda_{\text{em}} = 543$ nm; b1) Fluorimetric titration of **4b** ($\lambda_{\text{exc}}=478$ nm); b2) Experimental (●) and calculated (—) fluorescence intensities of **4b** at $\lambda = 550$ nm; c1) **4c** ($\lambda_{\text{exc}}=484$ nm); c2) Experimental (●) and calculated (—) fluorescence intensities of **4c** at $\lambda = 538$ nm; d1) **4d** ($\lambda_{\text{exc}}=484$ nm); d2) Experimental (●) and calculated (—) fluorescence intensities of **4d** at $\lambda = 548$ nm; e1) **4e** ($\lambda_{\text{exc}}=452$ nm); e2) Experimental (●) and calculated (—) fluorescence intensities of **4e** at $\lambda = 557$ nm



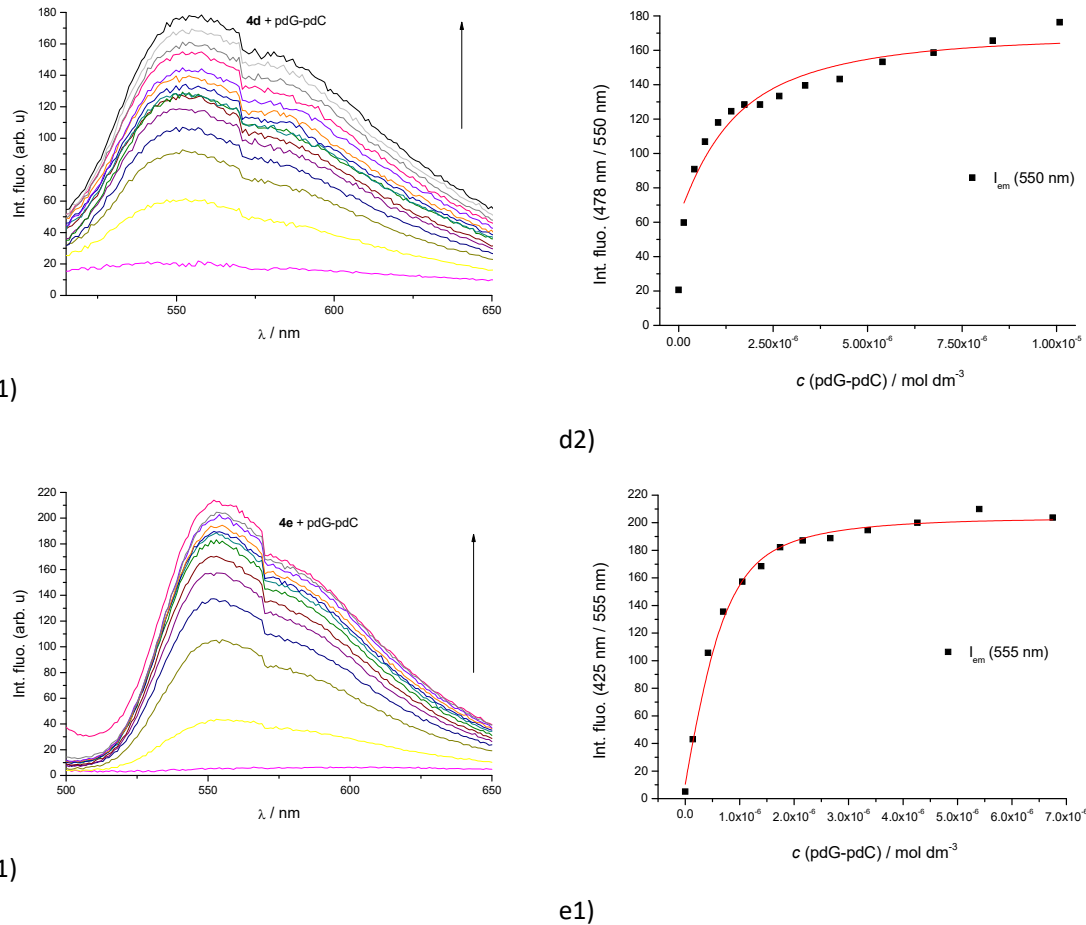
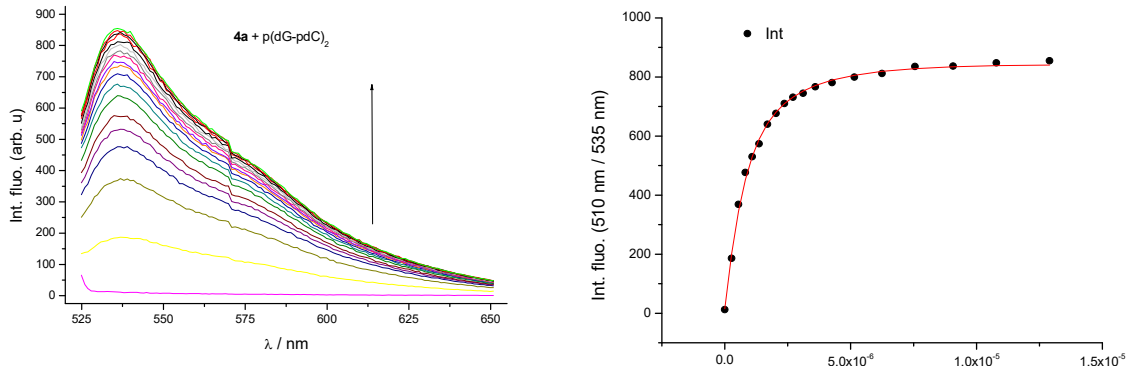
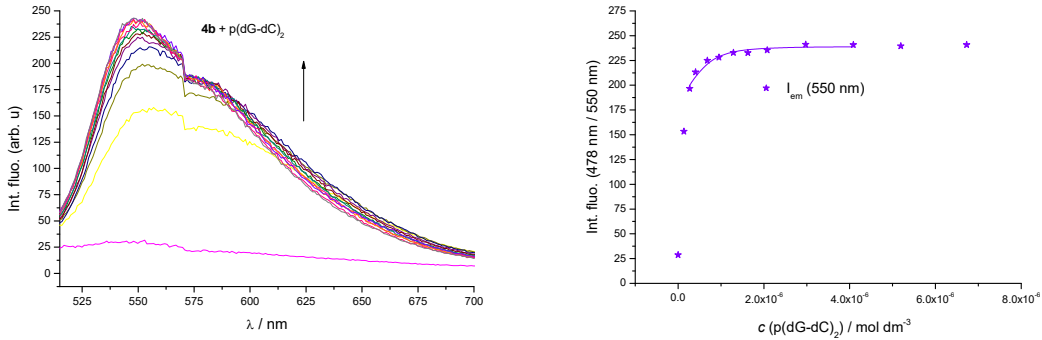


Figure S15. Fluorimetric titration of **4a-4e** compounds ($c = 1.3\text{-}1.5 \times 10^{-7}$ mol dm $^{-3}$) with **poly dG – poly dC**: a1) **4a** ($\lambda_{\text{exc}}=510$ nm); a2) Experimental (●) and calculated (–) fluorescence intensities of **4a** at $\lambda_{\text{em}} = 538$ nm; b1) Fluorimetric titration of **4b** ($\lambda_{\text{exc}}=478$ nm); b2) Experimental (●) and calculated (–) fluorescence intensities of **4b** at $\lambda = 550$ nm; c1) **4c** ($\lambda_{\text{exc}}=484$ nm); c2) Experimental (●) and calculated (–) fluorescence intensities of **4c** at $\lambda = 538$ nm; d1) **4d** ($\lambda_{\text{exc}}=484$ nm); d2) Experimental (●) and calculated (–) fluorescence intensities of **4d** at $\lambda = 550$ nm; e1) **4e** ($\lambda_{\text{exc}}=452$ nm) e2) Experimental (●) and calculated (–) fluorescence intensities of **4e** at $\lambda = 575$ nm



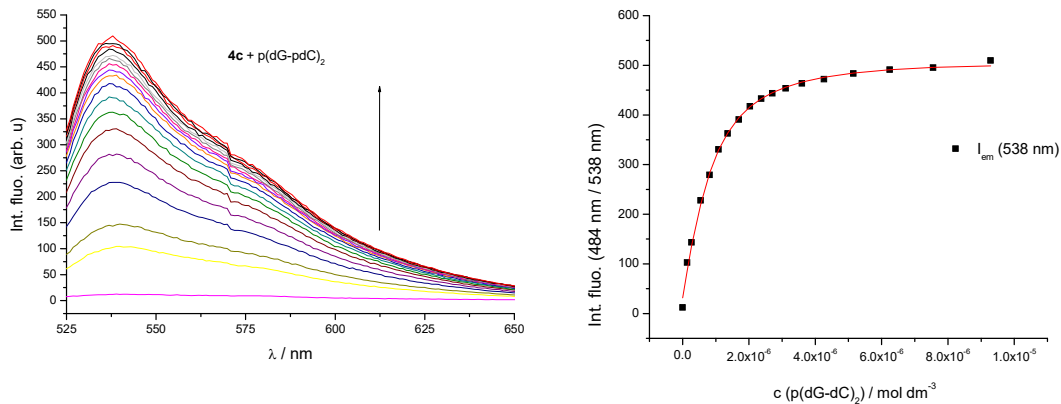
a1)

a2)



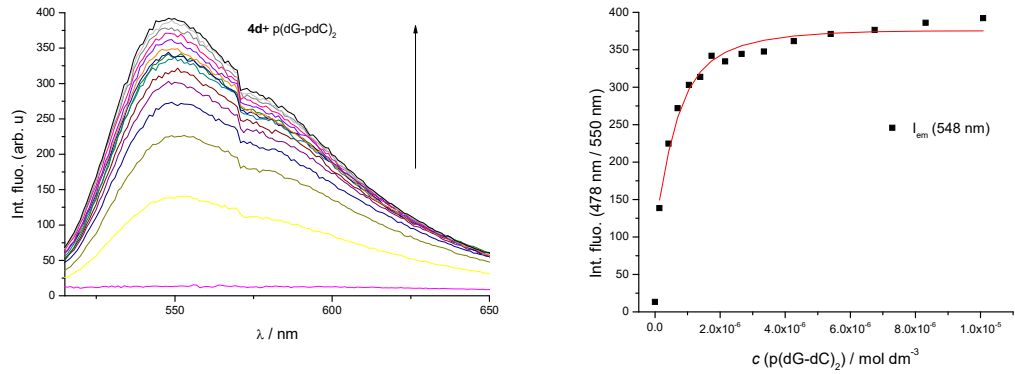
b1)

b2)



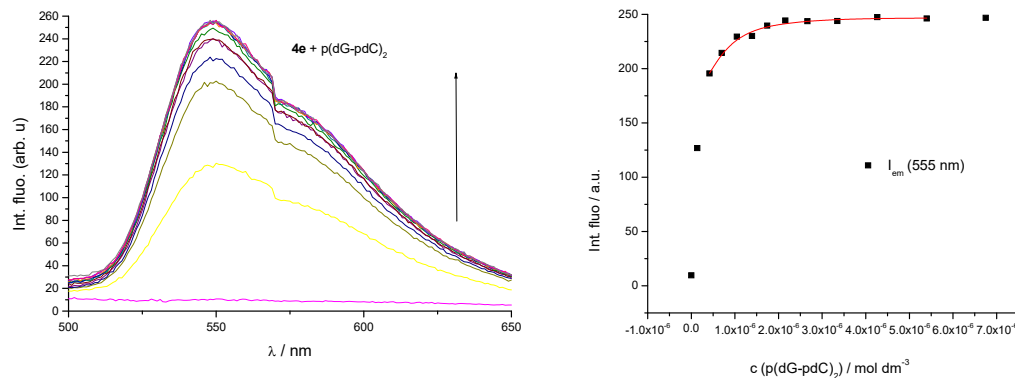
c1)

c2)



d1)

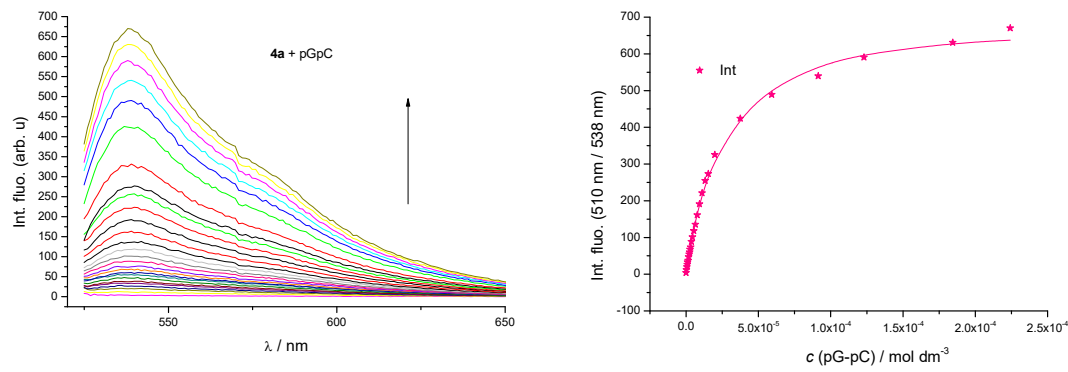
d2)



e1)

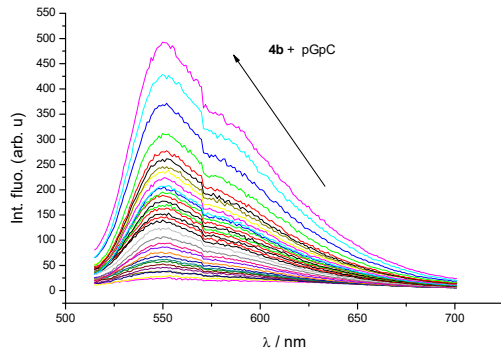
e1)

Figure S16. Fluorimetric titration of **4a-4e** compounds ($c = 1.3\text{-}1.5 \times 10^{-7}$ mol dm⁻³) with **polydGdC – poly dGdC**: a1) **4a** ($\lambda_{exc}=510$ nm); a2) Experimental (●) and calculated (—) fluorescence intensities of **4a** at $\lambda_{em} = 535$ nm; b1) Fluorimetric titration of **4b** ($\lambda_{exc}=478$ nm); b2) Experimental (●) and calculated (—) fluorescence intensities of **4b** at $\lambda = 550$ nm; c1) **4c** ($\lambda_{exc}=484$ nm); c2) Experimental (●) and calculated (—) fluorescence intensities of **4c** at $\lambda = 538$ nm; d1) **4d** ($\lambda_{exc}=484$ nm); d2) Experimental (●) and calculated (—) fluorescence intensities of **4d** at $\lambda = 548$ nm; e1) **4e** ($\lambda_{exc}=452$ nm) e2) Experimental (●) and calculated (—) fluorescence intensities of **4e** at $\lambda = 555$ nm

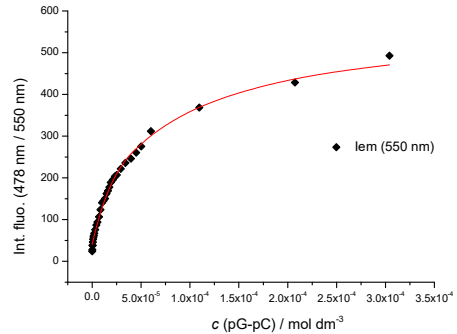


a1)

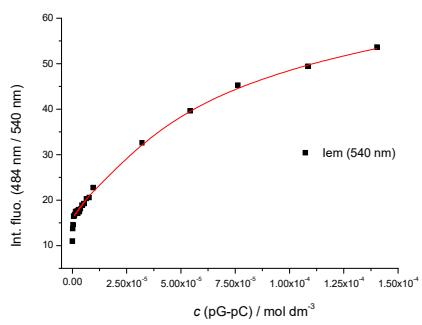
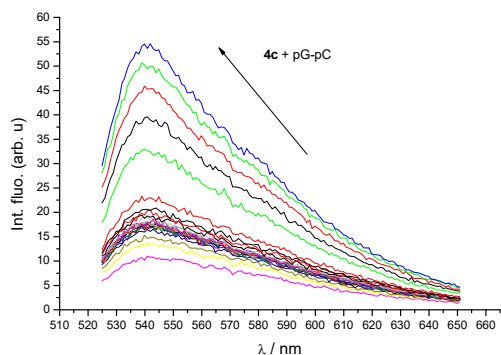
a2)



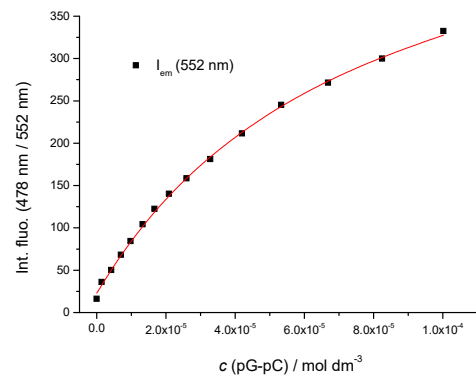
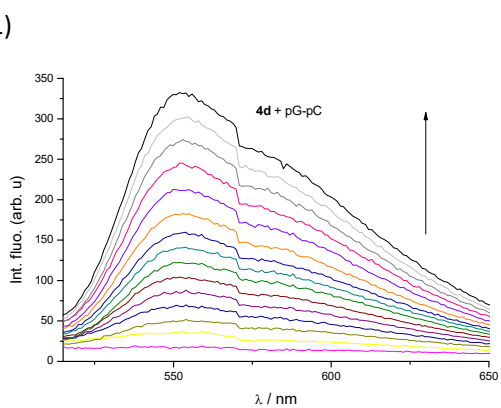
b1)



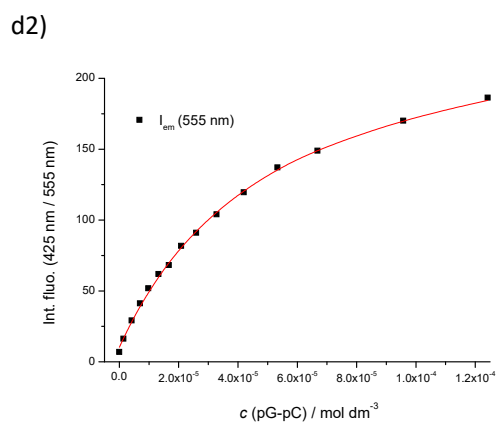
b2)



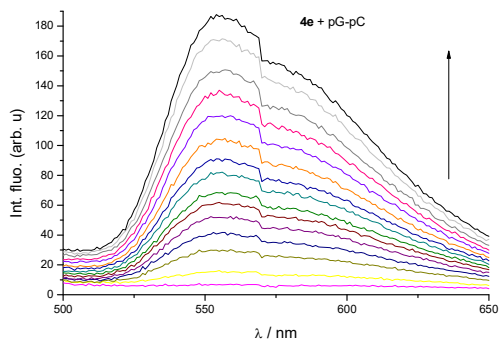
c2)



d1)



d2)



e1)

e1)

Figure S17. Fluorimetric titration of **4a**-**4e** compounds ($c = 1.3\text{-}1.5 \times 10^{-7}$ mol dm $^{-3}$) with **poly rG – poly rC**: a1) **4a** ($\lambda_{\text{exc}}=510$ nm); a2) Experimental (●) and calculated (–) fluorescence intensities of **4a** at $\lambda_{\text{em}} = 538$ nm; b1) Fluorimetric titration of **4b** ($\lambda_{\text{exc}}=478$ nm); b2) Experimental (●) and calculated (–) fluorescence intensities of **4b** at $\lambda = 550$ nm; c1) **4c** ($\lambda_{\text{exc}}=484$ nm); c2) Experimental (●) and calculated (–) fluorescence intensities of **4c** at $\lambda = 538$ nm; d1) **4d** ($\lambda_{\text{exc}}=484$ nm); d2) Experimental (●) and calculated (–) fluorescence intensities of **4d** at $\lambda = 548$ nm; e1) **4e** ($\lambda_{\text{exc}}=452$ nm) e2) Experimental (●) and calculated (–) fluorescence intensities of **4e** at $\lambda = 555$ nm

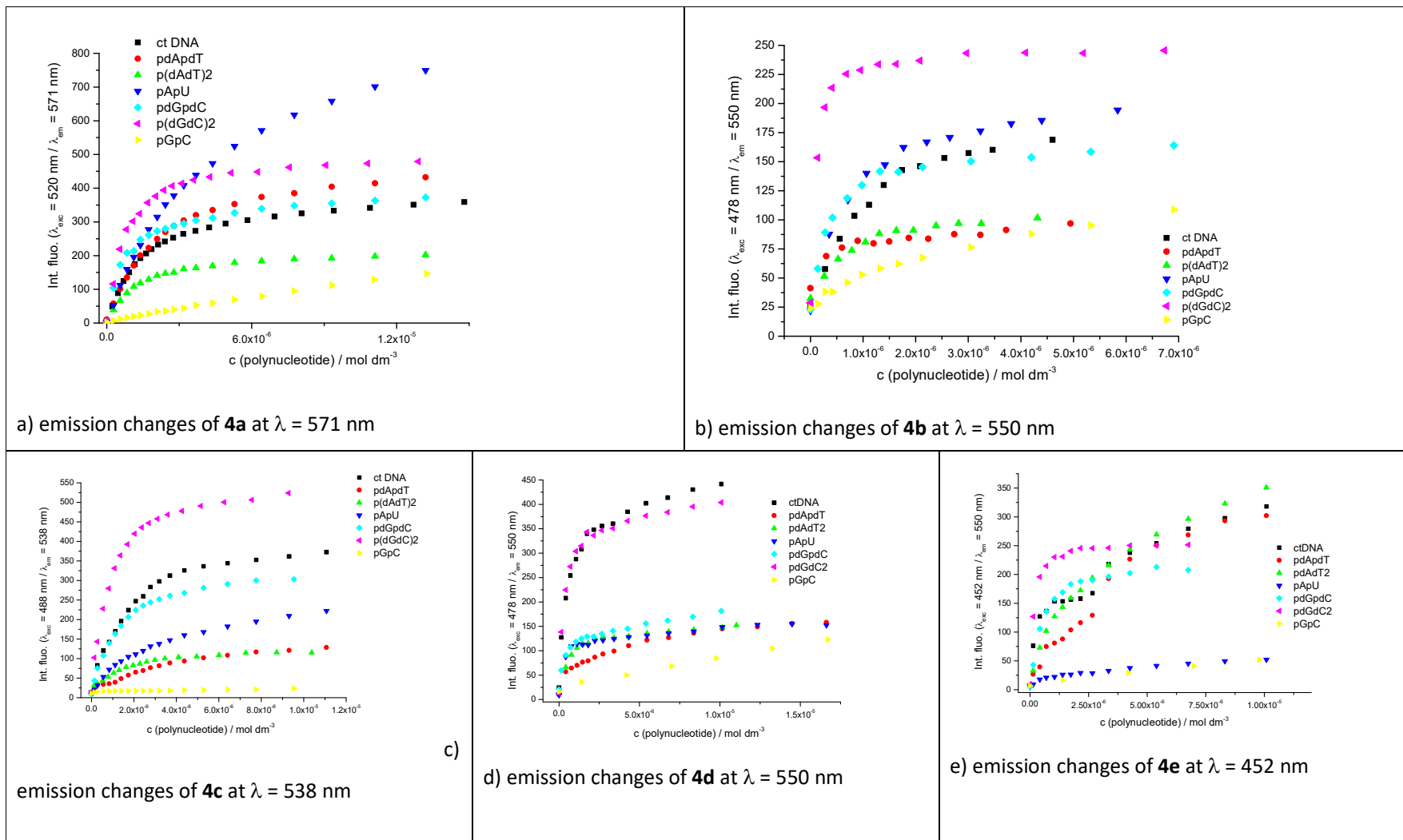
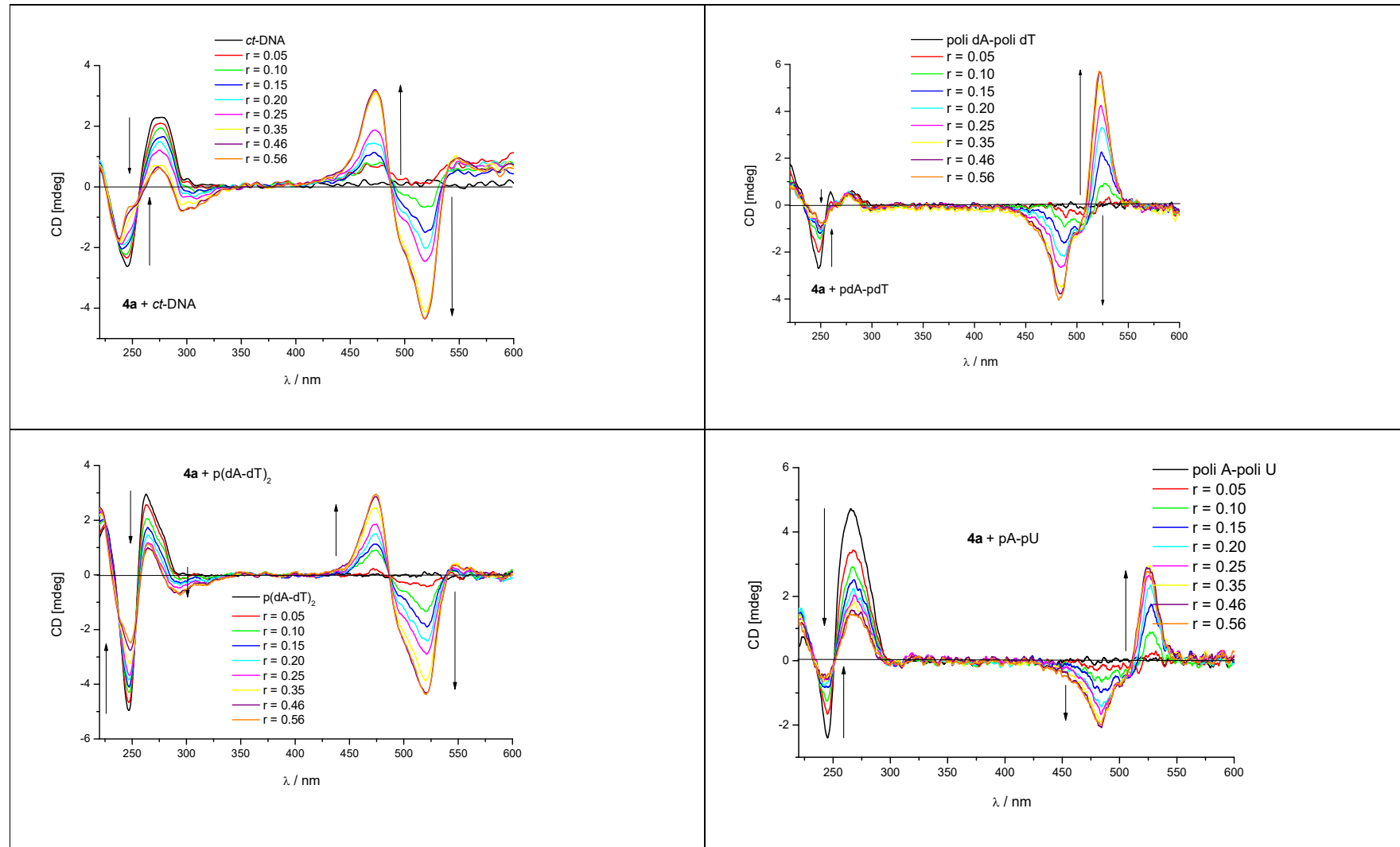


Figure S18. Changes of fluorescence emission at emission maxima of a) **4a** ($c = 1.3 \times 10^{-7}$ mol dm⁻³); b) **4b** ($c = 1.3 \times 10^{-7}$ mol dm⁻³); c) **4c** ($c = 1.48 \times 10^{-7}$ mol dm⁻³); d) **4d** ($c = 1.34 \times 10^{-7}$ mol dm⁻³); e) **4e** ($c = 1.34 \times 10^{-7}$ mol dm⁻³) upon addition of *ds*-polynucleotides at pH 7 (Na-cacodylate buffer, pH = 7.0, $I = 0.05$ M)

2.3. Circular dichroism (CD) experiments



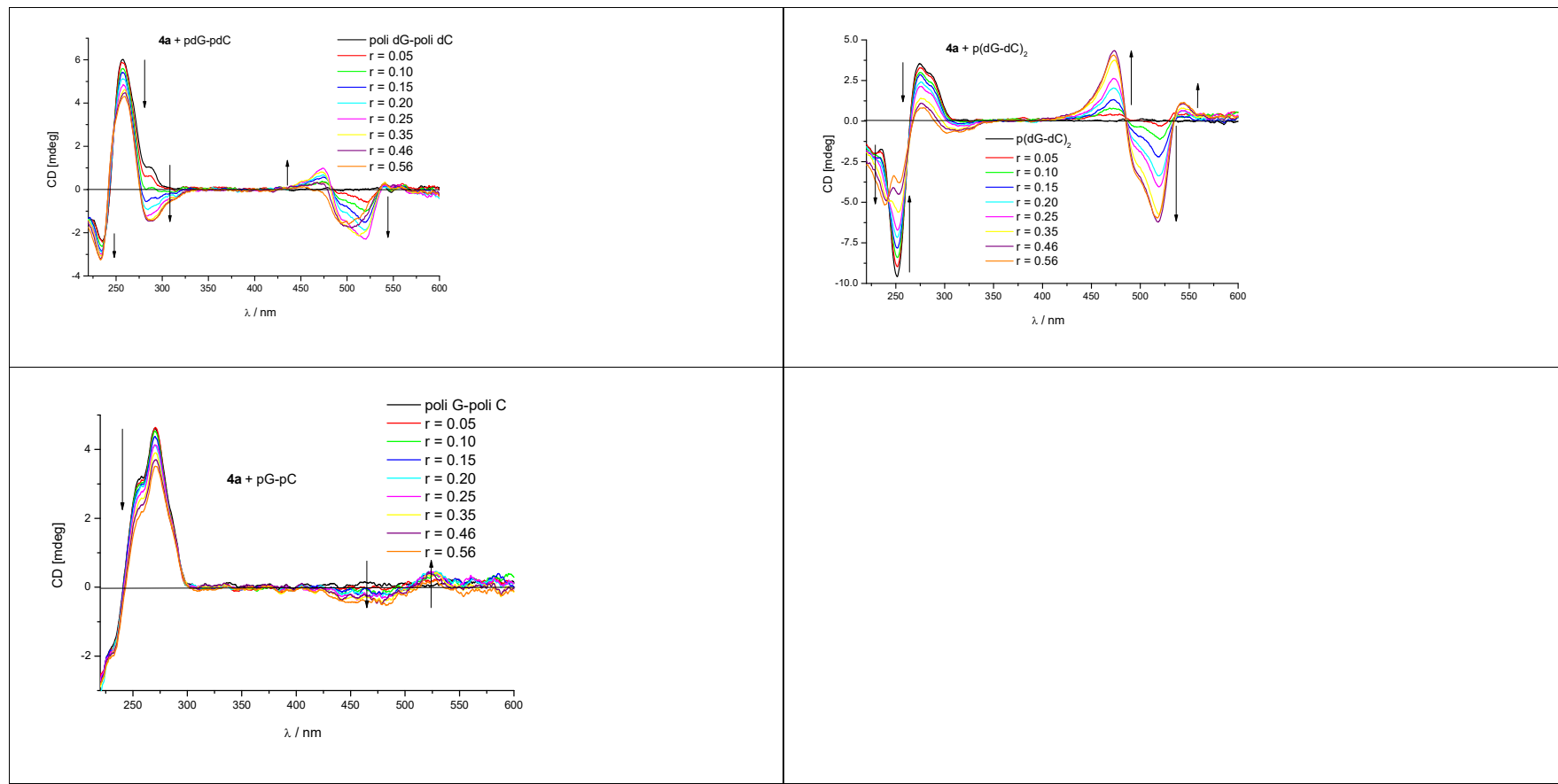
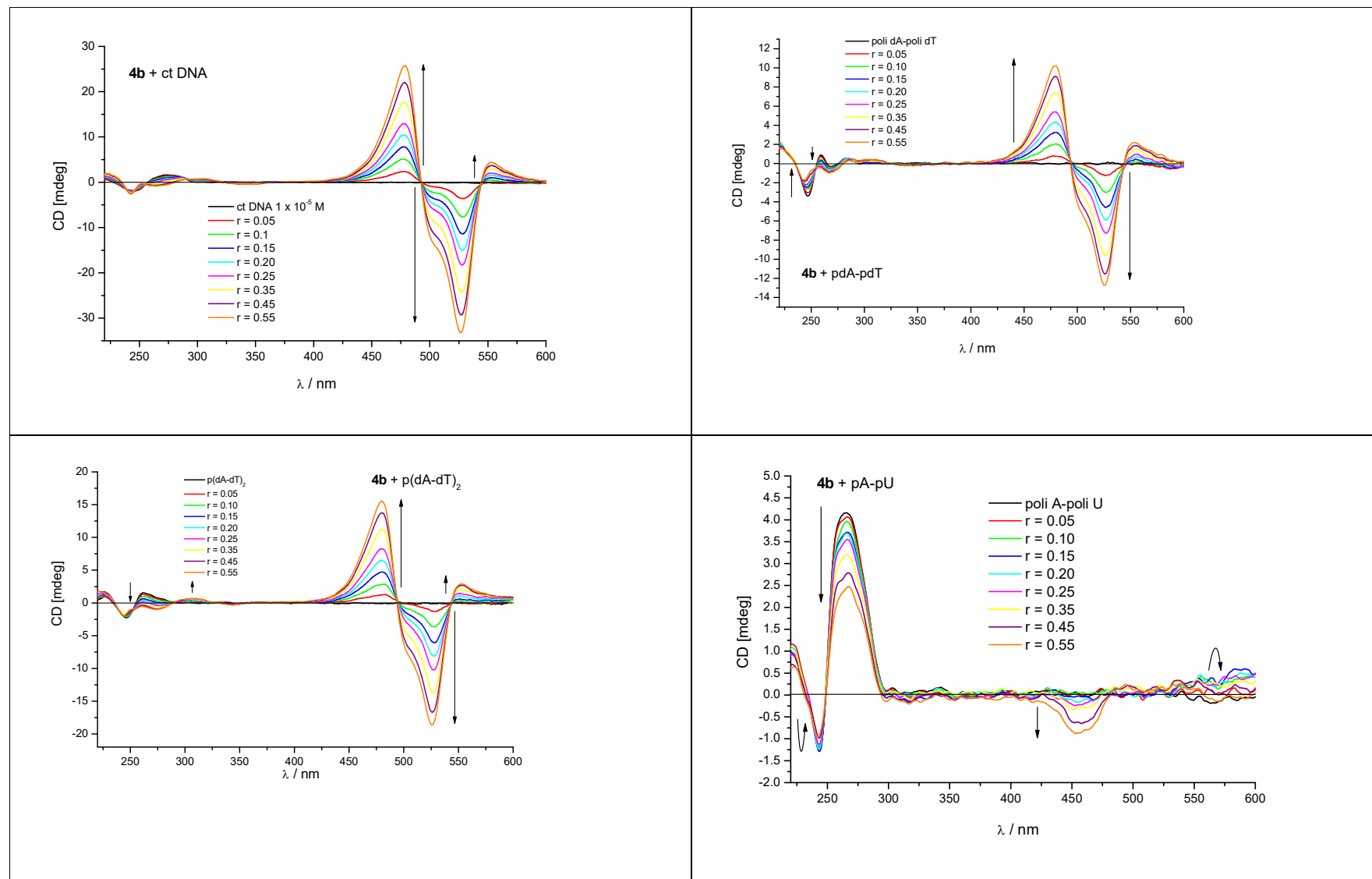


Figure S19. CD titration of polynucleotides ($c = 2.0 \times 10^{-5}$ mol dm $^{-3}$) with **4a** at different molar ratios $r = [\text{compound}] / [\text{polynucleotide}]$ (pH = 7.0, buffer sodium cacodylate, $I = 0.05$ mol dm $^{-3}$).



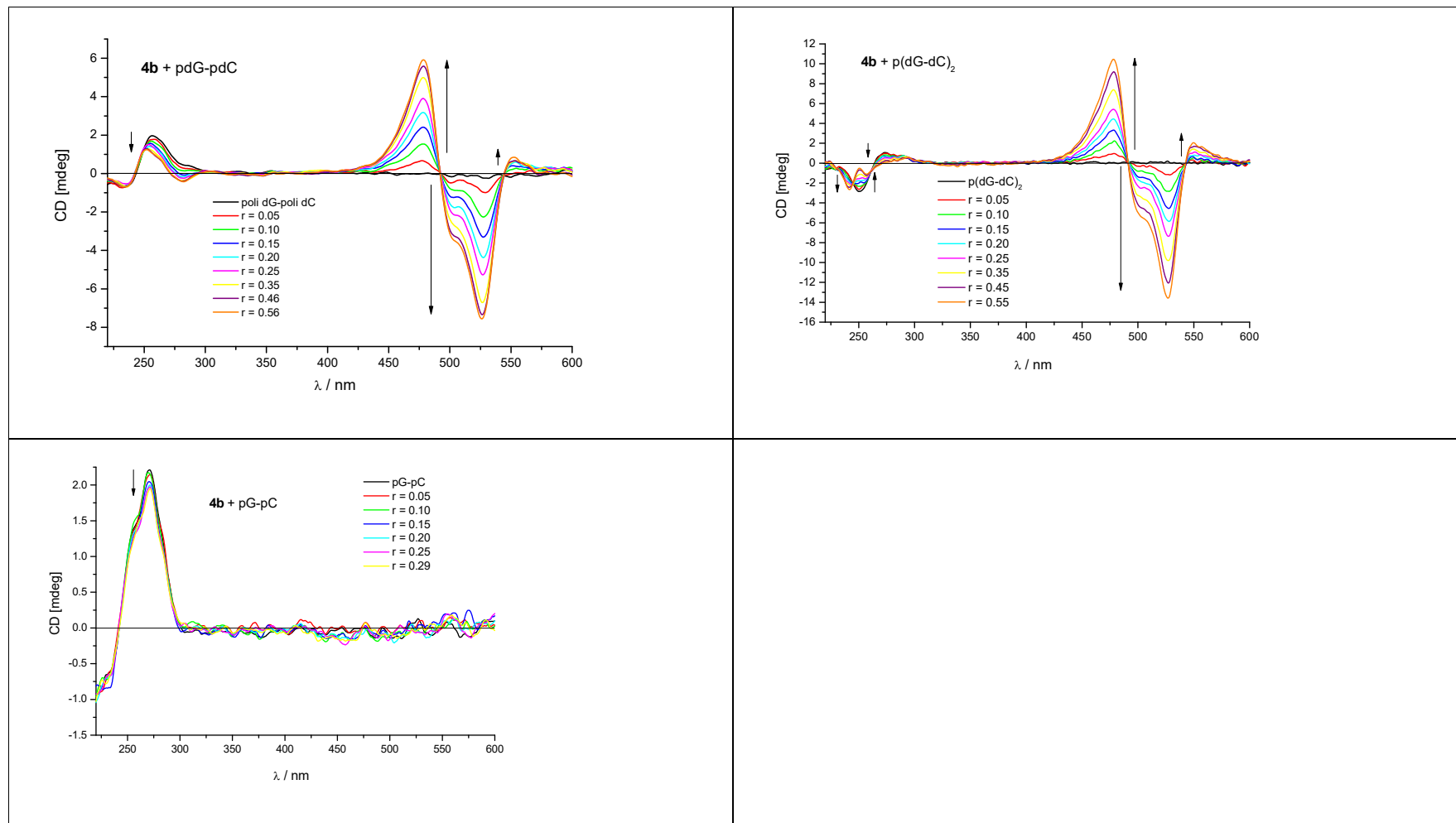
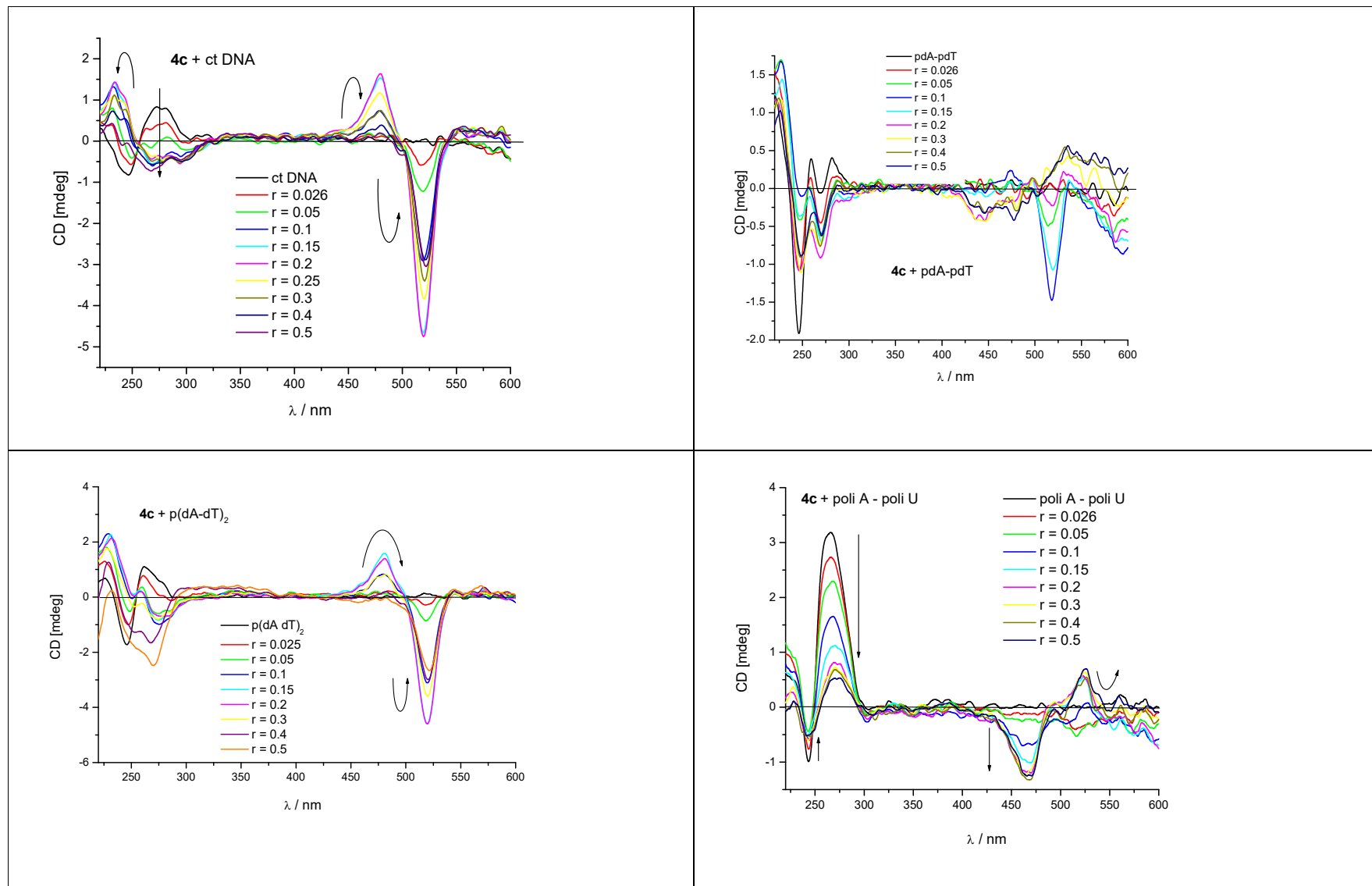


Figure S20. CD titration of polynucleotides ($c = 1.0 \times 10^{-5}$ mol dm $^{-3}$) with **4b** at different molar ratios $r = [\text{compound}] / [\text{polynucleotide}]$ (pH = 7.0, buffer sodium cacodylate, $I = 0.05$ mol dm $^{-3}$).



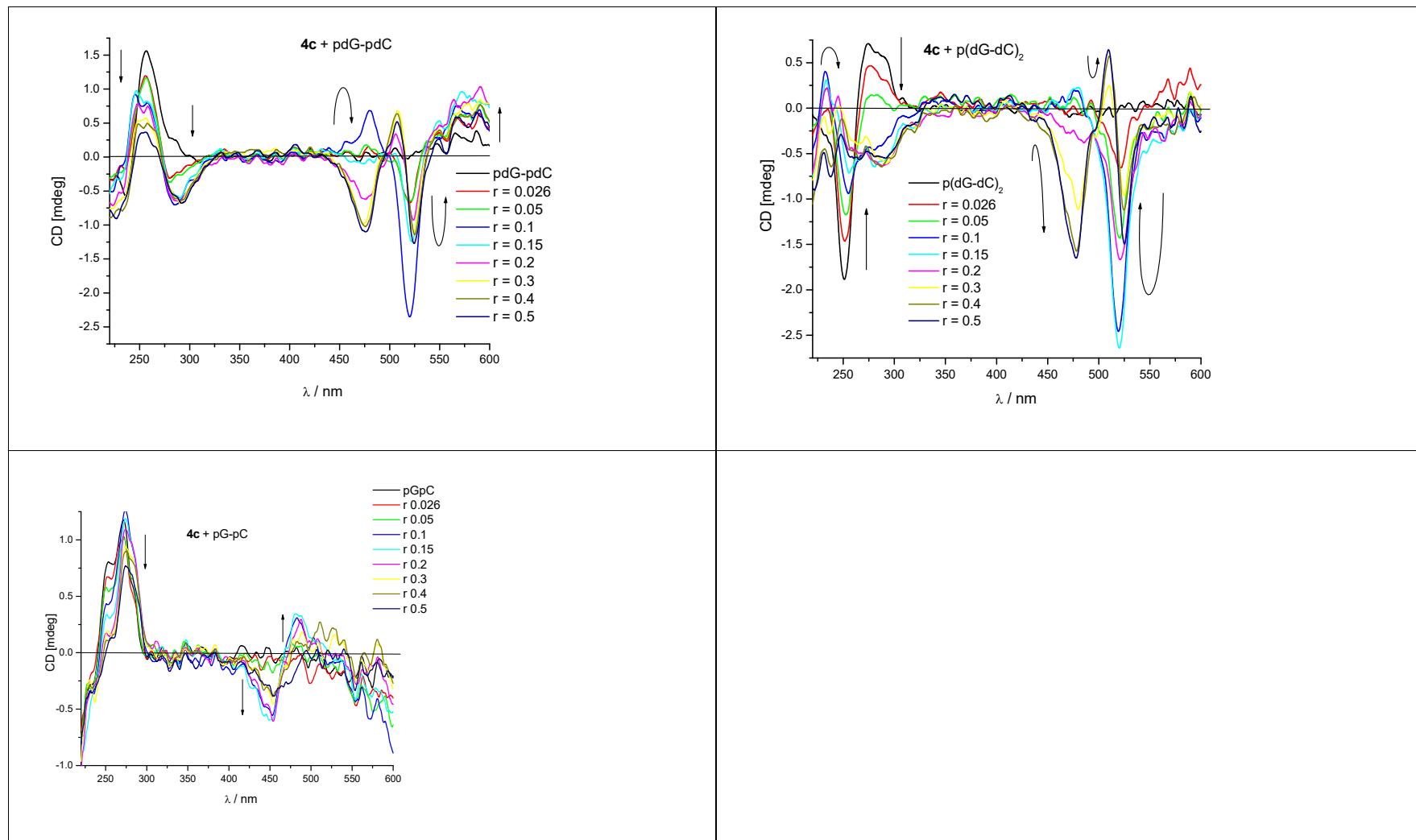
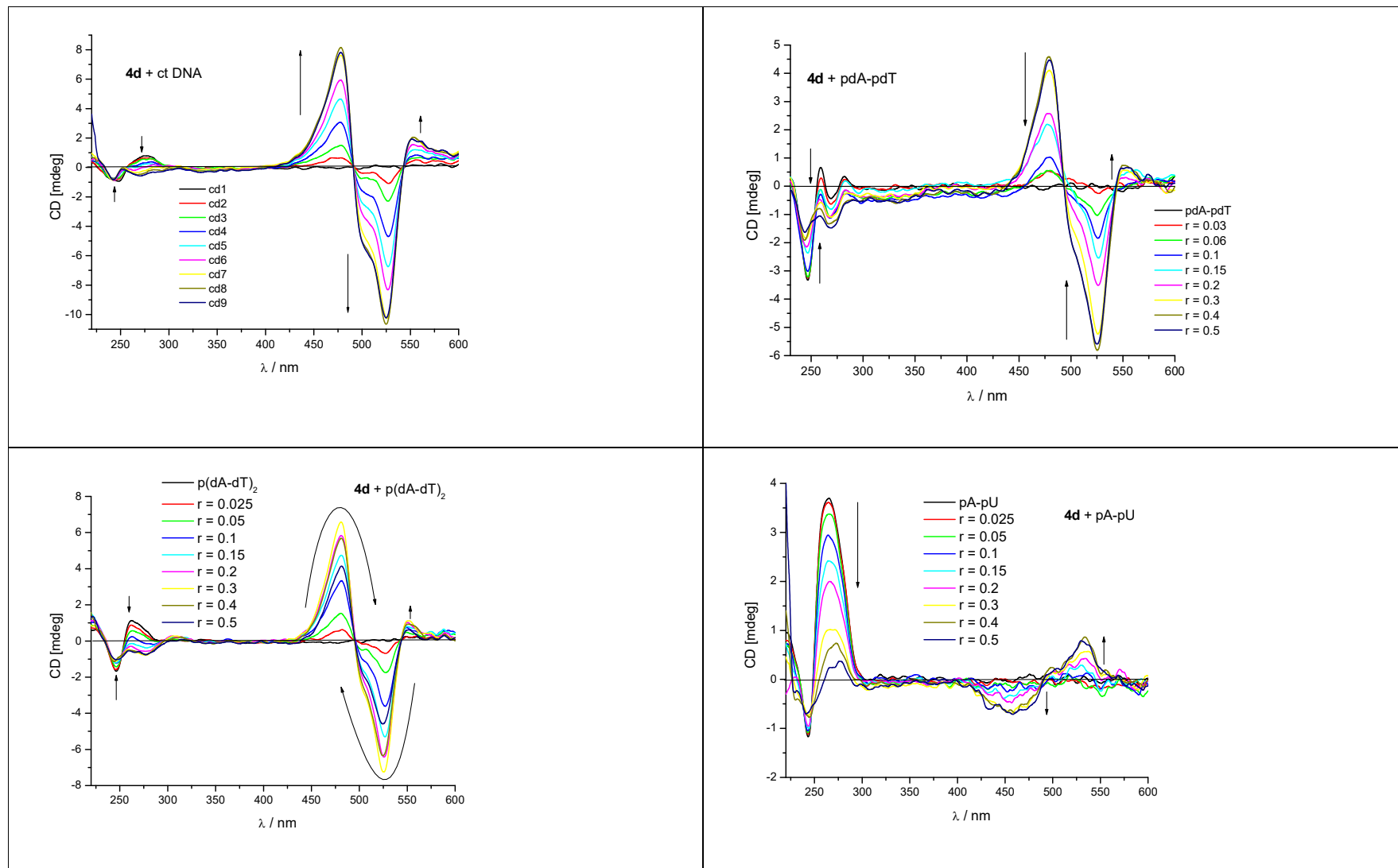


Figure S21. CD titration of polynucleotides ($c = 1.0 \times 10^{-5}$ mol dm $^{-3}$) with **4c** at different molar ratios $r = [\text{compound}] / [\text{polynucleotide}]$ (pH = 7.0, buffer sodium cacodylate, $I = 0.05$ mol dm $^{-3}$).



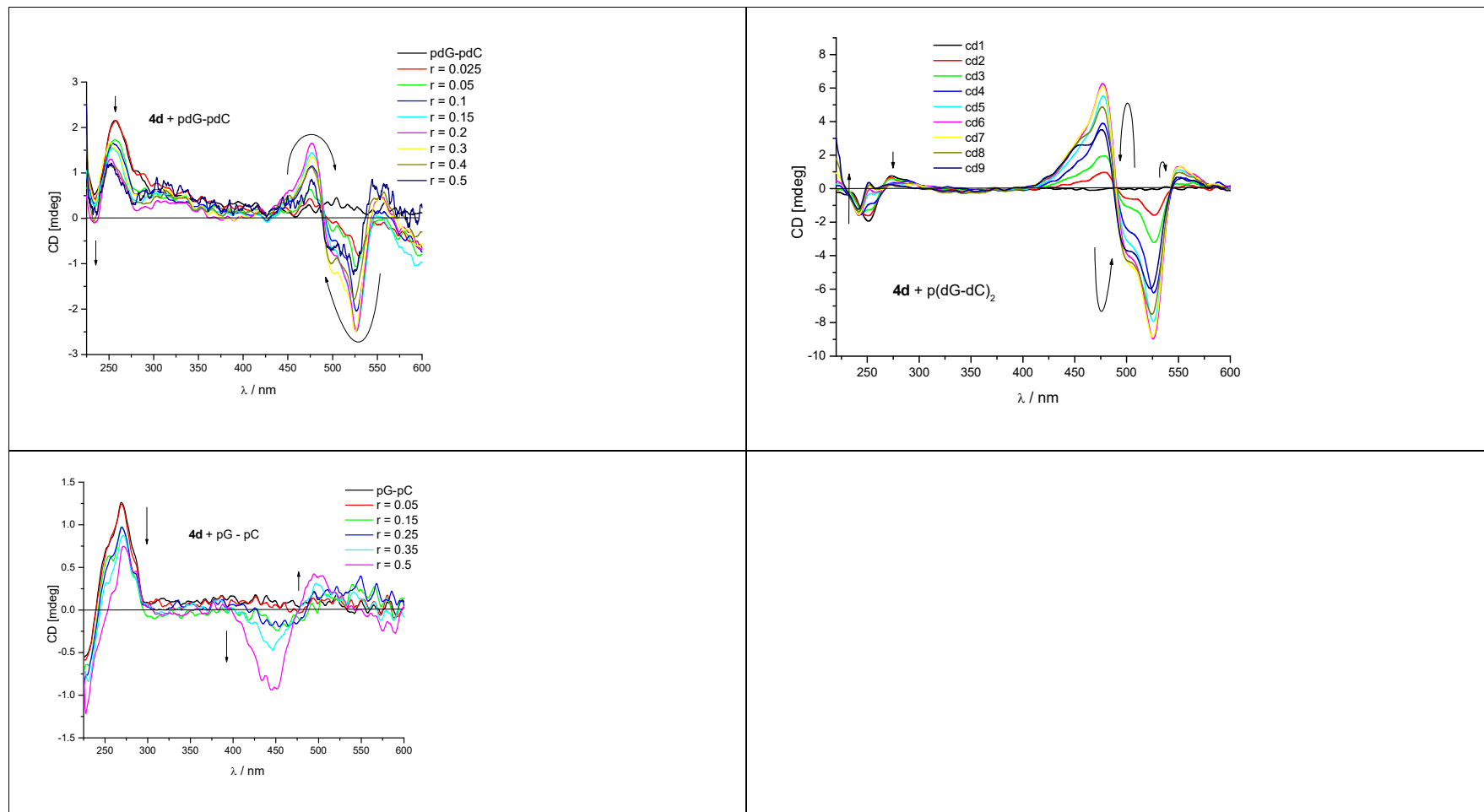
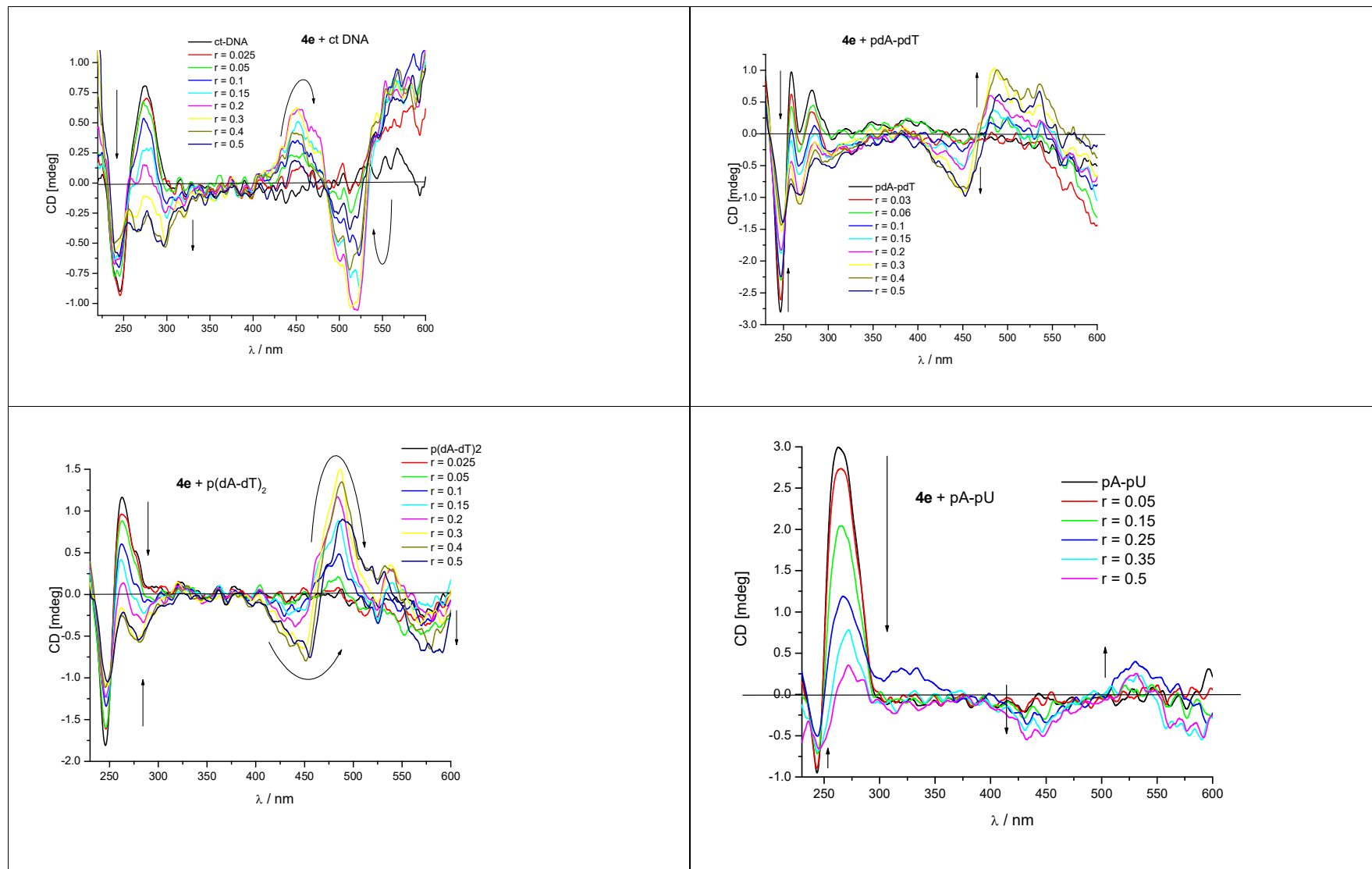


Figure S22. CD titration of polynucleotides ($c = 1.0 \times 10^{-5}$ mol dm $^{-3}$) with **4d** at different molar ratios $r = [\text{compound}] / [\text{polynucleotide}]$ (pH = 7.0, buffer sodium cacodylate, $I = 0.05$ mol dm $^{-3}$).



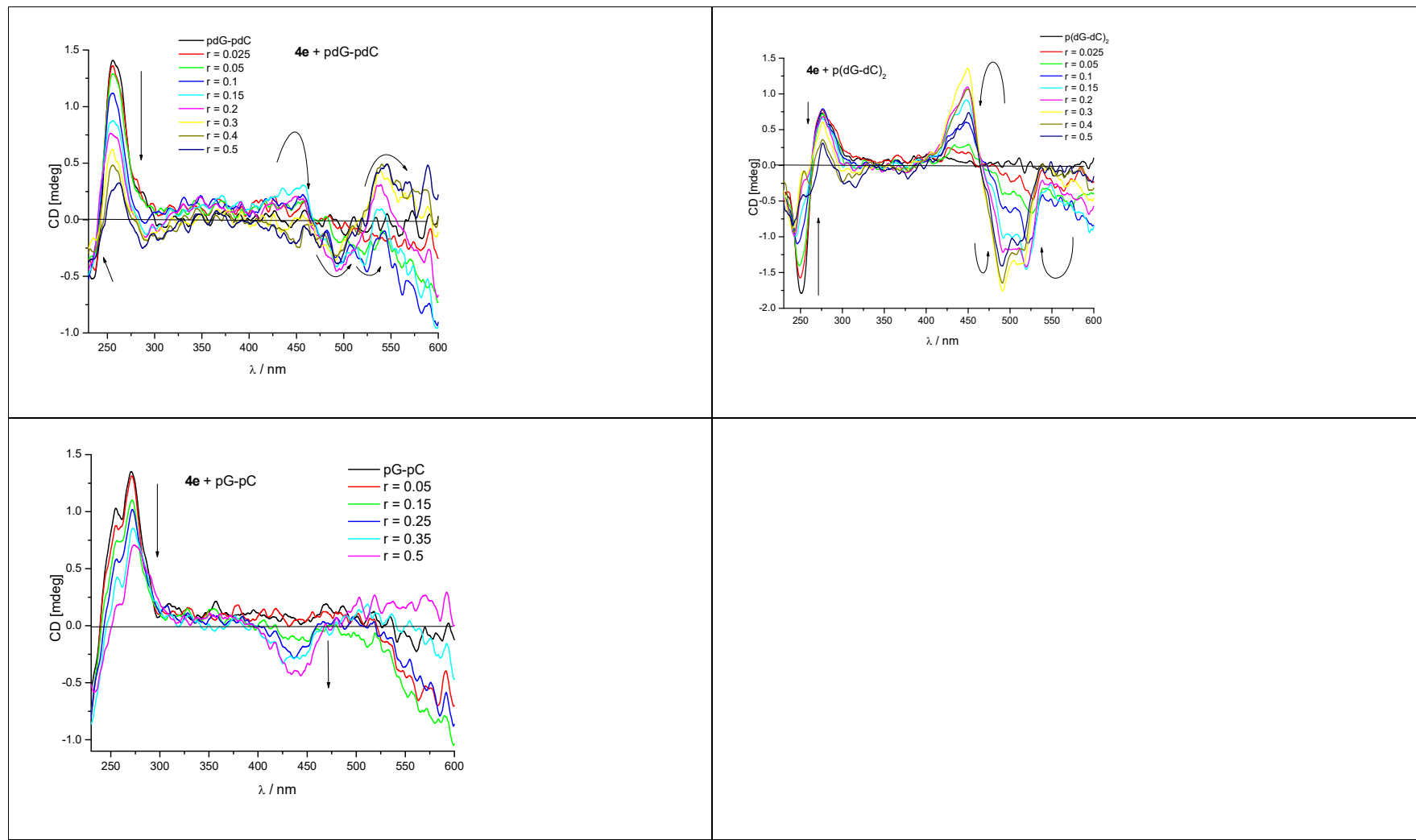


Figure S23. CD titration of polynucleotides ($c = 1.0 \times 10^{-5}$ mol dm $^{-3}$) with **4e** at different molar ratios r = [compound] / [polynucleotide] (pH = 7.0, buffer sodium cacodylate, $I = 0.05$ mol dm $^{-3}$).

3. Biological assays

The purpose of this study was to investigate the effects of compounds on the proliferation of different human tumor cell lines.

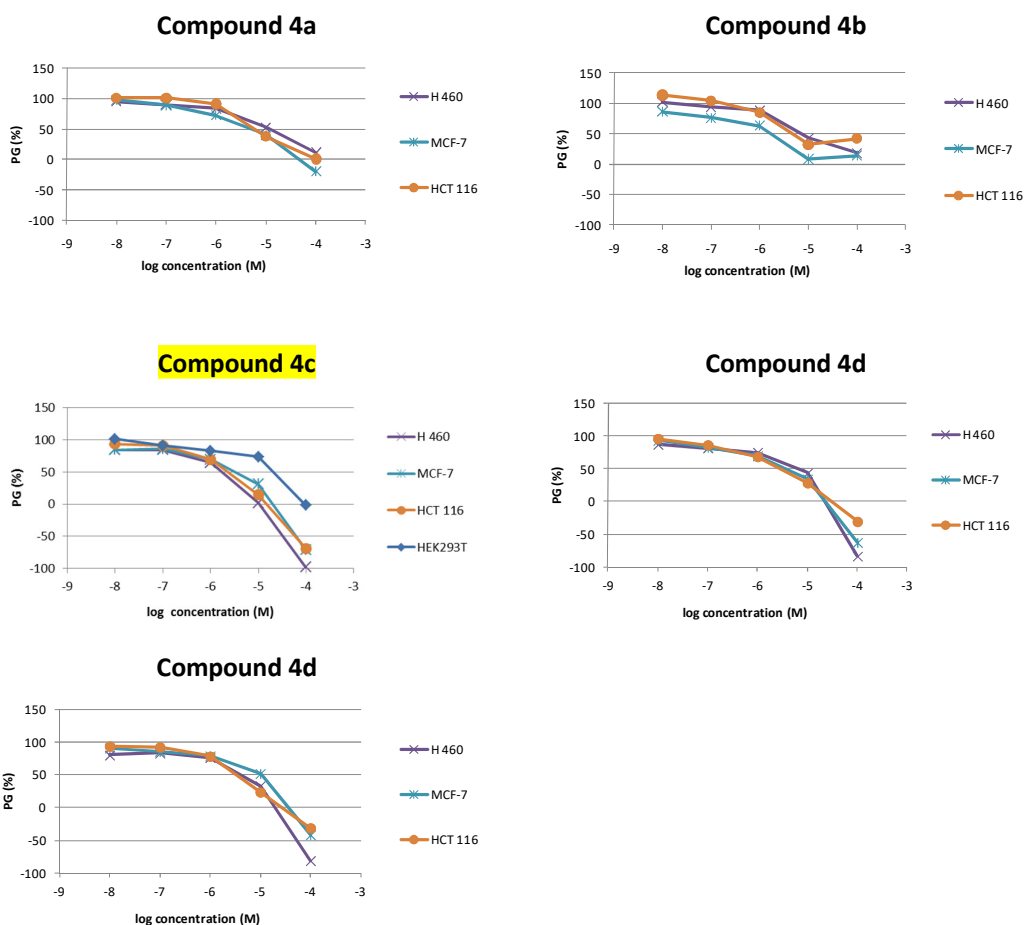


Figure S24. Dose-response profiles for compound 4a-4e compounds tested *in vitro*.

GI₅₀ and LC₅₀ calculations

The GI₅₀ measures the growth inhibitory power of the test agent and represents the concentration that causes 50% growth inhibition, while the LC₅₀ signifies a cytotoxic effect and represents the concentration that kills 50% of initial cell number. The GI₅₀ and LC₅₀ values for each compound are calculated from dose-response curves using linear regression analysis by fitting the test concentrations that give PG values above and below the respective reference value (e.g. 50 for GI₅₀). Therefore, a "real" value for any of the response parameters is obtained only if at least one of the tested drug concentrations falls above, and likewise at least one falls below the respective reference value. If however, for a given cell line all of the tested concentrations produce PGs exceeding the respective

reference level of effect (e.g. PG value of 50), then the highest tested concentration is assigned as the default value. In the screening data report, that default value is preceded by a ">" sign.

¹ W. Saenger, *Principles of Nucleic Acid Structure*, Springer-Verlag: New York, 1983; p. 226.

² G. Scatchard, *Ann. N.Y. Acad. Sci.*, 1949, **51**, 660-672.; J.D. McGhee, P.H. von Hippel, *J. Mol. Biol.*, 1976, **103**, 679-684.